AD-A167 693 SOUND ENHANCEMENT AND MODULATION OF SELF-RESONATING CAVITATING JETS FOR U..(U) TRACOR HYDRONAUTICS INC LAUREL MD G L CHAHINE ET AL. JUL 85 TRACOR-TR-83005-2 1/1

UNCLASSIFIED N00014-82-C-0678 F/G 20/1 NL

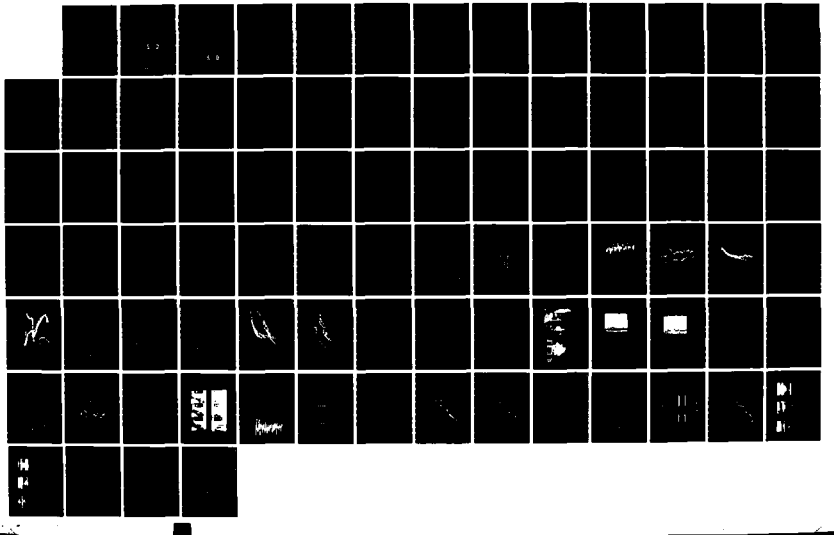

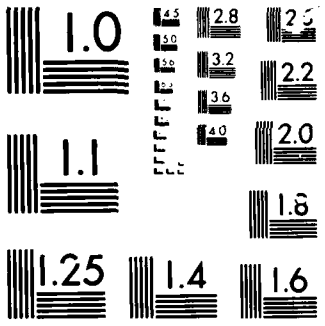

MICROCOPY CHART

(12)

SOUND ENHANCEMENT AND MODULATION OF SELF-RESONATING CAVITATING JETS FOR UNDERWATER NOISE GENERATION

BY

GEORGES L. CHAHINE
VIRGIL E. JOHNSON, JR.
GARY S. FREDERICK
AND
RON E. WATSON

JULY, 1985

Tracor Hydronautics, Inc.
[illegible] Laurel, Maryland 20707

(12)

Tracor Hydronautics

Technical Report 83005-2

SOUND ENHANCEMENT AND MODULATION OF SELF-RESONATING CAVITATING JETS FOR UNDERWATER NOISE GENERATION

BY

GEORGES L. CHAHINE
VIRGIL E. JOHNSON, JR.
GARY S. FREDERICK
AND
RON E. WATSON

JULY, 1985

The information in this report is based upon work supported by:

The Office of Naval Research
Department of the Navy
800 North Quincy Street
Arlington, Virginia 22217
Under
Contract No. N00014-82-C-0678

TABLE OF CONTENTS

FOREWORD AND ACKNOWLEDGMENTS

The study described in this report was conducted at Tracor Hydronautics, Inc., Howard County, Laurel, Maryland. This program was supported by the Office of Naval Research, Department of the Navy, under Contract No. N00014-82-C-0678. Some preliminary work related to this program as well as some of the fundamental studies related to it have been supported by Tracor Hydronautics' internal R&D funds. The CAVIJET® and STRATOJET™ technology used in this program has been patented by Tracor Hydronautics, Inc.*, and additional patent applications are being pursued.

We would like to thank many colleagues at Tracor Hydronautics for useful discussions and contributions during the execution of this program.

---

* U.S. Patents No. 3,528,704; 3,713,699; 3,807,632; 4,262,747; 4,389,071 and 4,474,251. Other U.S. and Foreign patents are pending or have been granted.

ABSTRACT

The natural tendency of an axisymmetric submerged jet to form large scale structures in its shear layer is enhanced using acoustic oscillators and hydroacoustic oscillations. Organ pipe tube lengths are tuned to the jet natural oscillation frequency to form very effective noise generators. The principle of operation of this generator, STRATOJET™, is described in this report, and the characteristics of the oscillations are presented. The influence of the various parameters: tube length, nozzle diameter, pressure drop across the nozzle, and ambient pressure are investigated. Scaling effects, cavitation influence on the oscillations, and characteristics of noise decay with distance are presented. The capability of modulation of the generated noise is investigated and its feasibility is demonstrated. Further improvement of the STRATOJET noise generation capabilities are studied. Several schemes aiming at manipulation of the ring vortex circulation are described. Opposing jets and solid enhancers were tested. Several solid enhancer configurations were found to be very effective, and amplification factors as high as 6 were measured without use of any additional energy. Even without enhancers, the efficiency of a STRATOJET is seen to be more than two orders of magnitude higher than that of conventional cavitating jets. This strongly suggests that a system based on a STRATOJET, possibly with an enhancement scheme, would be a very effective noise generation.

1.0 INTRODUCTION

Submerged jets that pulsate passively originally developed at Tracor Hydronautics for the purpose of enhancing the erosive action of jets in deep hole drill bits, have been shown during the execution of ONR Contract N00014-82-C0678 to be very effective underwater noise generators [1-4]. In these "STRATOJETS" (STructured, Resonating, Acoustically Tuned, Oscillating JETS) the passive excitation is obtained hydroacoustically and structures the shear layer of the jet into discrete, well-defined ring vortices when the excitation frequency, f, matches the jet's preferred frequency. The corresponding reduced frequency or Strouhal number, S_d, is usually in the range of 0.25 to 0.6. The large pressure oscillations associated with the intensification of cavitation, with the resonance in the nozzle assembly, and with the production and disappearance of ring vortical cavities are the source of the noise generated by these jets.

In the preceding Report [3] related to the present contract, the principle of operation of the STRATOJET as a sound generator was described and its main working characteristics were investigated experimentally. The main result will be summarized here. In addition, experiments investigating scaling effects, modulation of the generated sound and intensification of the emitted noise will be presented and discussed. These tests have demonstrated the capability of STRATOJETS to be used as signal modulators. In addition, solid plates or hole-tuned whistlers placed in front of the STRATOJET were investigated and were found to be effective sound enhancers. These enhancers are described in this report and the preliminary results of the investigations are presented.

2.0 PRINCIPLE OF OPERATION OF AN ORGAN-PIPE STRATOJET

The principle of operation and noise generation of an Organ-Pipe STRATOJET is schematically represented in Figures 1 and 2. Two predominant sources of pressure fluctuations can be distinguished besides the classical nonexcited turbulent shear layer between the jet and the surrounding liquid. One of these sources is easy to define and corresponds to the volume fluctuations of the moving vortex bubble rings formed in the center of the large structures of the self-excited jet. The other source of pressure fluctuations is more complex and relates to the exit region of the jet where high amplitude oscillations of the main flow characteristics are interrelated with the shear layer - nozzle lip interaction. This source behaves similar to an oscillating piston. Both sources of pressure fluctuations control simultaneously noise generation and the excitation of the resonator. As sketched in Figure 2, the acoustic signals from both areas are forcing functions to the resonating chamber in the nozzle assembly. These signals strongly interact, and they are both fed back and amplified by the organ-pipe of the STRATOJET and transmitted downstream to enhance jet structuring.

2.1 Main Frequency of the Emitted Noise

In an Organ-Pipe configuration, peak acoustic resonance is achieved when a standing wave forms in the "organ pipe" section of length L, and diameter D. This section is created by the upstream contraction from a plenum of diameter D_F and by the nozzle contraction, (D/d) (d is the nozzle diameter). Peak resonance will occur when the frequency of the organ-pipe wave is near the preferred jet structuring frequency. The exact resonance frequency is dependent on the contractions at each end

of the organ-pipe. For instance, if both (D_P/D) and (D/d) are large, then the first mode resonance in the pipe will occur when the sound wave length in the fluid is approximately four times L. When the contraction ratio D/d is close to one, resonance occurs when the wave length is approximately two times L.

Therefore the frequency of the emitted noise of an Organ-Pipe STRATOJET is mainly determined by the length of the organ-pipe chamber, L. Actually, due to end corrections, the effective length of the pipe is longer, and

$$f \approx \frac{c\ K_n}{L\ (1+\beta)} \quad . \tag{1}$$

The "mode parameter," K_n is given, for $D_P/D \gg 1$, by

$$K_n = \text{func}\ (n, \frac{D}{d}, M) \approx \begin{cases} \frac{2n-1}{4}; & \text{for } \frac{D}{d} > \frac{1}{\sqrt{M}} \quad , \qquad (2) \\ \frac{n}{2}\ ; & \text{for } \frac{D}{d} < \frac{1}{\sqrt{M}} \quad , \qquad (3) \end{cases}$$

In these expressions n is the mode number of the organ-pipe, M is the jet Mach number ratio of the average velocity of the jet, V, to the speed of sound in the liquid, C, and β is an end correction for the organ-pipe length [5].

2.2 Optimum Operating Jet Velocity

Optimum performance of the STRATOJET is achieved when the resonance frequency of the Organ-Pipe matches the jet preferred frequency. This latter corresponds to a Strouhal number, S_d, close to 0.3 or its integer multiples. Acoustic analysis and experimentation have led to the following approximation, useful

for estimating the length of the organ-pipe for relatively low Mach numbers:

$$M = \frac{K_n}{2 S_d} \left[\frac{d}{L} - 0.86 \left(\frac{d}{L}\right)^2 \right] , \qquad (4)$$

where S_d is the critical Strouhal number, $S_d = fd/V \approx 0.3n$. Figure 3 shows a diagram of optimum Mach numbers for different jet diameter to organ-pipe length ratios. In fact strong resonance occurs in a range of values of the velocity which are centered on the value given by Equation (4).

3.0 EXPERIMENTAL FACILITIES

A small test cell was used for evaluations of the resonance characteristics of the noise generator and to ensure that the designed nozzle was feeding back large flow oscillations in the pipe. The test chamber was a clear acrylic cylinder with aluminum end plates, and an inside diameter of 28 cm (11 in.). A small positive displacement pump served to pressurize the test cell up to 1.1 MPa (160 psi). A centrifugal pump took suction directly from the test cell and discharged through a flexible hose into a plenum feeding the STRATOJET assembly. The flow through the pump, up to 4.5×10^{-3} m/s (65 gpm), was regulated by a discharge valve to effect the desired nozzle pressure drop, up to 0.5 MPa (75 psi). Very good visualization of the jet structuring and characterization of the pressure oscillations in the organ pipe tube were afforded by this facility. However, no reliable noise measurements could be made in the cell because of its relatively small size.

A second cell connected to the same pump supply was used to study opposing jets. This chamber was also cylindrical in shape and made of clear acrylic sides. The inside diameter was about 18 cm (7 in.) and the length about 85 cm (33.5 in.). The axis of the cylinder was positioned horizontally and matched the axis of the two opposing STRATOJETs mounted on each end plate of the cell. This facility was used for flow visualization and organ pipe oscillations characterization of the interaction between two identical jets.

For actual noise measurements, the STRATOJET systems were tested in a facility larger than those described above. In order to minimize reflections, avoid standing waves in the range of

frequencies of interest, and be able to vary the degree of cavitation for constant jet velocity, we used the Hydronautics Ship Model Basin. The basin is 128 m long, 7.6 m wide, and 4 m deep. In addition, the presence in this basin of a well 13 m deep, and 3.35 m in diameter (see Figure 4) allowed us, by locating the nozzle at various depths, to control the ambient pressure at the nozzle exit. This enabled us to vary the cavitation number while keeping the jet velocity constant without the drawbacks of a small enclosed tank and wall reflections. A diesel-driven portable quintuplex pump, which allowed a maximum flow rate of 5.7 l/s (90 gpm) and a maximum pressure of 17.2 MPa (2,500 psi) was used.

As schematically shown in Figure 5, the nozzle assembly tested for noise generation consisted of a plenum feeding a straight stainless steel pipe of length L. This pipe, which acted as an organ pipe, discharged into the ambient liquid through a nozzle having a hemispherical shape with a sharp edge. The nozzle lip was shaped and sized such as to provide a feedback of the preferred natural frequencies of the jet oscillations to the organ pipe which amplified them. The lip consisted of a cylindrical section of length e, followed by a conical bevel of length t. Five nozzle sizes were tested. Their exit diameters were 0.5, 0.75, 1, 1.25, and 1.5 cm (0.2, 0.3, 0.4, 0.5, and 0.6 in.) measured at the cylindrical section diameter. For all cases studied in this report, the dimensions for e and t were chosen to be d/2, and the bevel angle was 45°.

A pressure transducer located at the midpoint of the organ pipe allowed comparison between the pressure oscillations in the pipe and the noise measurements in the field surrounding the jet. The pressure transducer was a Piezotronic ICP Model 101M55,

with resonant frequency of 250 kHz. A KSP UT-114 hydrophone, having a practically flat response up to 30 kHz and ±4db oscillations up to 100 kHz, was used to measure the acoustic pressure at different locations away from the nozzle. Both signals were applied to a TSI Model 1060 RMS voltmeter and a Hewlett Packard 3580A frequency analyzer whose limit frequency was 50 kHz. A Nicolet memory oscilloscope and X-Y plotter were also used to observe the signals and to record the instrument outputs. These signals were usually filtered below 60 Hz to eliminate undesirable noise.

4.0 TYPICAL STRATOJET OSCILLATION CHARACTERISTICS

The acoustic pressure p_h', detected by a hydrophone located at a field point $M(r,\theta)$ (see Figure 5) is, for a given nozzle geometry, a function of several geometrical and flow characteristics. This can be written, by considering only the predominant variables, as follows:

$$\frac{p_h'}{\Delta P} = f\ (r/d,\ \theta,\ R_e,\ \sigma,\ S_d,\ M,\ \text{geometry}\ \ldots) \quad , \qquad (5)$$

where, in addition to the nondimensional parameters defined earlier, Re is the Reynolds number based on the nozzle diameter, and σ is the cavitation number defined as the ratio between the difference between the ambient pressure, Pa, and the vapor pressure, Pv, and the pressure drop across the nozzle, ΔP, $\sigma = (Pa-Pv)/\Delta P$. This functional relation is, a priori, unknown and it is practically impossible to vary independently one parameter at a time, except for the position of the microphone $(r/d,\ \theta)$. This interdependency turned out to be the major problem for the scaling tests (Section 5.0). Some general aspects of the signals generated and the main features of the functional relation of Equation (5) have been investigated and are presented in this section.

4.1 General Sound Characteristics

Figure 6 shows an example of the detected pressure fluctuations with the hydrophone and the pressure transducer. From these raw signals it is evident that while the transducer senses only the oscillations main frequency, the hydrophone detects both the main fluctuations in the organ pipe and the

high-pressure spikes due to growing and collapsing cavitation vortex rings. This is made clearer when one considers Figures 7 and 8. Both figures compare the frequency spectrums of the signals detected by the hydrophone and the transducer. While the main frequency of oscillation of the organ pipe ($\approx$600 Hz in this case) is predominant in both spectrums (Figure 7), the higher end of the spectrum ($f > 30$ kHz) is of rich content only for the hydrophone (Figure 8). For the user interested only in the low frequencies, this remark seems of little importance; however, one should note that since the frequency of occurence of the high-pressure high-frequency pressure spikes matches the main frequency of oscillations of the Organ Pipe, these spikes strongly influence the energy content of this main frequency. These pressure spikes also act as sources of excitation and feed-back to the Organ Pipe oscillator.

4.2 Influence of the Cavitation Number

The direct influence of cavitation on the Organ Pipe acoustic oscillations indicates the importance of the cavitation number, σ, on the generated sound. Jet structuring and system resonance are also affected by the degree of cavitation for the following reasons: a) the jet's predominant natural frequency (Strouhal number) is a strong function of σ (see Jorgensen [6]); b) the secondary flow in the nozzle lip area is greatly influenced by the degree of cavitation, and feedback could be totally suppressed if developed cavitation occurs inside the lip.

Figures 9 and 10 are typical examples of the variations of acoustic pressure oscillations with the cavitation number. Figure 9 shows the pressure flucuations for a 1 cm diameter nozzle (0.4 in.) when the jet velocity was fixed and the ambient

pressure continuously varied. This test was conducted in the visualization cell where a relatively large range of values of σ was achieved. The general trend was as follows: the rms values of the generated noise - which were practically constant for high values of σ or of the ambient pressure - were singularly disturbed when the value of σ approached the inception value. A dramatic increase of the acoustical performance of the noise generator was observed when cavitation occurred (see, for example, the pressure jump at $\sigma \simeq 1.01$, for $\Delta P \simeq 0.286$ MPa (41.5 psi). A discrete frequency corresponding to the organ-pipe natural frequency was then emitted. This can be explained by the fact that the cavitation events occurred at a rate corresponding to the "preferred" frequency of the jet structuring and thus at a frequency matching the organ pipe natural frequency. Since the amplitude of the fed-back forcing function corresponding to these bursts was much higher than that of the noncavitating case, the organ pipe response and the noise generated by the STRATOJET were much higher.

At the lower end of the observed values of the cavitation number, a dramatic drop of the acoustic pressures was observed. This was probably due to the formation of a large vapor cavity at the nozzle exit in the straight region of the lip of length e, which prevented a good feedback into the organ pipe. A similar behavior was observed even at high values of the cavitation number when e was too large.

In addition to the general trends explained above, Figure 9 shows the complexity of the phenomena due to the multiplicity of the variables. The curves for different values of ΔP follow the same trends and show optimum performance of the noise generator in the same range of values of σ. However, scaling effects are

obviously present. Changing the jet velocity (Mach number) influences the amplitude of the oscillations as well as the values of the cavitation number at which the STRATOJET begins to resonate. This explains the scatter observed in the data obtained with different nozzle sizes that is presented in the following section.

4.3 Influence of the Jet Velocity

Figure 10 shows, for a fixed ambient pressure, the influence of the jet velocity (or Mach number) on the pressure fluctuations. Here again, changing the pressure drop across the nozzle modifies simultaneously the Mach number, the cavitation number and the Reynolds number. This figure shows a typical result obtained in the deep well of the Towing Tank. The depth of submergence was fixed and the pressure drop across the nozzle, ΔP, was continuously varied. The value of ΔP was monitored using a differential pressure transducer. This pressure difference and either the rms readings of the transducer located at midlength of the pipe or of the hydrophone fixed at a given distance from the nozzle were fed to an x-y plotter. Figure 10 shows the existence of several values of the Mach number at which the STRATOJET performance peaks. These values, when corrected for the influence of the cavitation number, correspond to the different modes of oscillations of the organ pipe represented in Figure 3. As can be seen in Figure 10, the first mode ($\Delta P \simeq 0.24$ MPa $\simeq 35$ psi) is that having the highest amplification rate, $\bar{p}_h'/\Delta P$ or $\bar{p}'/\Delta P$. (The amplification rate is given by the slope of the line joining the origin of coordinates to the considered point on the curve.) Interpretations of the transducer reading were complicated by its fixed location. For instance, the second mode of oscillation ($\Delta P \simeq 0.55$ MPa $\simeq 80$ psi in that case) was almost

undetected since the transducer was essentially at an oscillation node. The hydrophone located in the farfield was insensitive to these differences and gave a more accurate and direct measurement of the noise produced.

4.4 Sound Decay With Distance

Theoretical considerations as well as experimental observations have shown that the self-resonating jet behaves in the far field as an oscillating spherical radiator. The pressure fluctuations, $\bar{p}'$, at a distance r from the nozzle, are then related to the pressure drop, ΔP, across the nozzle by the relation:

$$\frac{\bar{p}'}{\Delta P} = \alpha \cdot \frac{d}{r} \qquad (6)$$

where

$$\alpha = \frac{\pi}{2} \cdot S_d \cdot \frac{\bar{v}'}{V} \quad . \qquad (7)$$

$\bar{v}'$ is the rms velocity fluctuations at the nozzle exit and V is the average jet velocity. Maximizing α is the objective when designing an efficient STRATOJET. This is also true for the acoustic efficiency η of the jet, given by the ratio of radiated sound power to hydraulic power

$$\eta = \frac{P_s}{P_h} = 8 \alpha^2 \cdot M \qquad (8)$$

Figure 11 compares the attenuation of the acoustical noise generated by two STRATOJETs and that generated by a conventional cavitating jet. The anticipated decay given by Equation (6) is

observed. For the better of the two nozzle presented here, the value of α is 0.18. This indicates a velocity fluctuation at the nozzle exit $\bar{v}'/V \simeq 0.4$. For conventional cavitating nozzles, such as the classical renowned study of Jorgensen done at NSRDC [6], α has a value an order of magnitude lower. As a result, the acoustic efficiency, η, of a STRATOJET is largely superior to a conventional cavitating nozzle. Using the relationship (8) between η and α, one finds:

$$\eta \simeq 0.26\ M \quad , \tag{9}$$

for the 1 cm diameter STRATOJET nozzle (0.4 in.), and

$$\eta = 0.093\ M \quad , \tag{10}$$

for the 0.5 cm diameter nozzle (0.2 in.). Jorgensen reports for a conventional cavitating nozzle

$$0.0005\ M < \eta < 0.003\ M \quad . \tag{11}$$

These values for conventional cavitating jets, an order of magnitude higher than for non-cavitating jets, were two to two and a half orders of magnitude lower than the efficiency of the STRATOJET used in the experiments shown in Figure 11. In terms of decibels, the 1 cm diameter nozzle, working at a pressure drop of 0.35 MPa (52 psi), or at a jet velocity of 30 m/s (90ft/s), generated about 183 db/ref 1 μPa at a distance of 1 meter. This value can be increased by increasing nozzle diameter, pressure across the nozzle, and by improving the nozzle efficiency with better design. For instance if Relation (6) holds, 12 db could be gained if the operating velocity is doubled or the jet diameter multiplied by four. However, the scaling laws need to

be checked for the possibility of this extension. This is the object of the following sections.

5.0 SCALING EFFECTS

A large set of nozzle diameter - Organ Pipe length combinations were investigated in the Hydronautics Ship Model Basin. Table 1 is a compilation of the main characteristics of the significant tests conducted. Two different approaches have been considered in studying the effect of nozzle size. In the first approach, the length of the Organ Pipe was kept constant and therefore the frequency of the sound generator remained the same. In the second approach, the frequency was allowed to change and geometric scaling was sought. With this approach and based on Equation (4) all nozzle sizes should produce peak oscillations at the same Mach and Strouhal numbers. Unfortunately as seen below, the neglected factors, such as the Reynolds number, and more importantly, the geometric scale factor related to the secondary flow field in the nozzle lip area introduced important effective scaling factors. One of the major problems encountered during the scaling study was the unexpected large sensitivity of the generated pressure fluctuations to the finer details of the nozzle lip geometry. This materialized during testing by the occasional need to modify the length of the nozzle lip, e, (see Figure 5) or to sharpen the angle between the two sections e and t, in order to achieve the expected large oscillations with a newly constructed nozzle. For the same reason, the peaks in the curves of relative pressure fluctuations, $p'/\Delta P$, versus the pressure drop across the nozzle, ΔP, were difficult to repeat especially when these peaks were sharp (corresponding to a range of values of ΔP not large compared with the precision of the control of the pump pressure). Similarily, these peaks were hard to locate when the nozzle size was changed. This was partly due to the particular nozzle shape chosen for this study. Other nozzle shapes developed in projects conducted in parallel with

this study [7, 8] have proven to be less sensitive to small variations in ΔP. Thus, interpretation of the collected data is complicated due to the influence of many variables on a given set of tests, and to the large sensitivity of the results to these variables.

5.1 Influence of the Cavitation Number

As discussed earlier, and illustrated in Figure 9, pressure fluctuations are significantly high only in a range of values of the cavitation number σ. At the very low values the feedback mechanism is lost, probably because of vapor filling the separated area in the nozzle lip. At the very high values cavitation does not take place. This results in a reduction of flow fluctuations since cavitation is a major source of resonator excitation for the nozzle types tested in this study. One of the results obtained in this study is that at constant frequency of resonance (same organ pipe length) an increase in the nozzle diameter reduces the upper limit value of σ before the loss of strong oscillations. This can be seen in Figures 12 and 13 where three nozzles of 1, 1.25, and 1.5 cm diameters (0.4, 0.5, and 0.6 in.) and an organ pipe length of 1.12 m (44 in.) are compared. A fourth nozzle of diameter 0.5 cm (0.2 in.) with a 55.9 cm (22 in.) organ pipe length is also shown in these two figures. As discussed earlier, more than one parameter has changed from one case to another. For instance, changing the nozzle diameter while keeping the rest of the geometry the same, also modifies the optimum nozzle pressures which generate high fluctuations. We believe, however, that the major effects are due to the modification of the nozzle contraction ratio. Keeping the same organ pipe diameter and increasing the nozzle diameter reduces the contraction ratio and therefore the relative spacing between

the jet shear layer and the nozzle lip wall in the separated region. Since the lip shape is optimized with the nozzle of diameter 1 cm (0.4 in.), the lip length has to be modified accordingly when the contraction is changed. For smaller contractions the ratio of lip length to nozzle diameter should be reduced. Figure 12, which is based on the signal detected by the transducer located at mid length of the organ pipe, seems to indicate only small changes between various nozzles of the same organ pipe length in the low σ range. However, when the organ pipe length is changed a shift of the overall $\bar{p}'/\Delta P$ versus σ curve is observed. Figure 13, shows the pressures detected by the hydrophone located at about 60 nozzle diameters for the same cases as in Figure 12. The same comments as above apply to the hydrophone signals except for a lower sensitivity the cavitation number variations in the high amplitude oscillations region.

Figure 14 and 15 analyze in more detail the range of cavitation numbers which correspond to large oscillations. A detailed preliminary discussion of this region has been given in our previous report [3] for the two nozzles of diameter 0.5 cm and 1.0 cm (0.2 and 0.4 in.). Extensive additional tests have been conducted since (see Table 1). Both the previous and the new results are shown in Figures 14 and 15. One should realize that interpretation of these figures is quite difficult. At first glance the data seem scattered. However, it could be regrouped in two band-curves. These could be related to the relative location of the transducer with respect to the wave shape. The transducer located for all tests at midlength of the pipe sensed the largest oscillations when this position corresponded to a maximum in the pressure wave form. For the case $L \simeq 3\lambda/4$ the transducer is closer to a pressure node. Some of the results cannot be explained except by a probable defect in the nozzle

shaping. Unfortunately, time and budget did not allow for the repetition of these tests. For instance, in Figure 14, if one considers the three geometrically scaled nozzles 0.5, 0.75, and 1.0 cm (0.2, 0.3, and 0.4 in., Tests No. 22, 25, and 28), the results are surprising. The curves of the nozzles of diameter 0.5 cm and 1.0 cm (0.2 and 0.4 in.) collapse, which is expected, while the results of the 0.75 cm (0.3 in.) diameter nozzle are totally different. Similarily ΔP at the peak is about the same for the 0.5 and 1.0 cm (0.2 and 0.4 in.) nozzles, while it is very different for the 0.75 cm (0.3 in.) nozzle. This again seems to indicate a deviation from design of the nozzle shape. The data from the other nozzles seem to fall on the same S-shaped curve, the region of largest scatter being in the drop-off part of the curve. This is observed when the measuring transducer is located at a pressure antinode. In the other cases, such as $d \simeq$ 0.5 cm (0.2 in.) and $L \simeq 56$ cm (22 in.) $\simeq 3\ \lambda/4$, data points fall on a lower $\bar{p}'/\Delta P$ curve. A discussion on this facet of the problem has been given in [3]. The influence of the contraction ratio d/D, can be seen for the case $d \simeq 0.5$ cm (0.2 in.), $L \simeq$ 56 cm, (22 in.). Apparently changing the nozzle contraction introduces a shift in the oscillations mode. For this particular case the oscillatons move from $L \simeq \lambda/2$ to $L \simeq 3\lambda/4$.

Figure 15 shows, for the same test cases as in Figure 14, the response of a hydrophone located at a sixty radii distance from the nozzle. Here again the scatter in the data can only be explained by the nozzle performance shifting from one mode to another or from strong to weak oscillations. The data seems to fall on one of the two ranges of values of $\bar{p}_h'/\Delta P$; either about 0.5 percent or 0.25 percent.

5.2 Sound Decay With Distance

As in Figure 11 Figure 16 shows the decay function of the generated noise with distance from the nozzle. In Figure 11 the point of optimum performance for each nozzle was chosen. However, the depth of submergence of 1.7 m (5.5 ft) was selected only because in the Model Basin this depth is practical for the measurement of pressure oscillations at a wide range of distances from the nozzle with no wall reflection problems. For this reason the cavitation number could not be the same for the two nozzles. A different pressure drop across the nozzle would have been needed for the 0.5 cm (0.2 in.) nozzle. The source nature of the noise generator, at the locations of observation, was observed. The rms value of the acoustic pressure detected by the hydrophone decayed with the distance r from the nozzle as 1/r. The data falls within the experimental errors on the drawn lines, $y = \alpha d/r$. The measured value of α for the conditions presented in Figure 15 was for $\theta \leq 60°$:

$$\alpha \simeq 0.18, \text{ for } d \simeq 1 \text{ cm},$$
$$\alpha \simeq 0.11, \text{ for } d \simeq 0.5 \text{ cm}. \qquad (12)$$

The difference between these two values is related to the acoustical performance of the two nozzles as influenced by the cavitation number as explained above and illustrated by Figure 12. For $\theta = 90°$ the value of α drops to 0.06 for the 0.5 cm (0.2 in.) nozzle. Even then the acoustical performance of the self-resonating nozzle is several times better than a nonresonating cavitating jet [6]. Expressed in terms of the coefficient α such jets would have the value

$$0.008 < \alpha < 0.02. \qquad (13)$$

Figure 16 is a continuation of Figure 11. The decay function of the pressure fluctations with the distance r from the orifice is shown for seven different nozzles. The data is shown here in dimensional form in order to compare the effective noise generation characteristic of each of the nozzles. As underlined above, there is unfortunately some doubt about the perfect similitude of the nozzles. The conclusions we can draw are therefore tentative. Five of the nozzles have shown peak oscillations at a value of the pressure drop across the nozzle between 0.358 and 0.414 MPa (52 and 60 psi). It appears from Figure 16 that d ≈ 1.0 cm (0.4 in.) gave the best results. The expected tendency of p' to increase, at a given distance from the orifice, with the nozzle diameter seems to apply between 0.5 cm and 1.0 cm (0.2 and 0.4 in.). However for the higher values 1.25 cm and 1.5 cm (0.5 and 0.6 inches), the tendency is reversed. The only explanation we can find is the reduced value of the nozzle contraction ratio for these two last nozzles which destroys similitude of the separation region in the nozzle lip and therefore the conservation of the feedback mechanism similitude. The two other nozzles of diameter 1.0 cm and 0.5 cm (0.4 in. and 0.2 in.) and of pressure drop at peak oscillation of 0.662 and 0.234 MPa (96 psi and 34 psi), illustrate typical cases of nonsimilar nozzles. Probably, errors in the nozzle fabrication have changed the value of the pressure drop at peak oscillations. These errors have evidently reduced the acoustic emission properties of the 1.0 cm (0.4 in.) nozzle. However, the differences between the two 0.5 cm (0.2 in.) nozzles can be explained by the difference in ΔP at peak oscillation.

Additional experimentation in which particular attention is paid to accounting for nozzle shape sensitivities and to tightly controlling fabrication of these sensitive regions should be able to confirm these tentative conclusions. Investigations could also be carried out with nozzle designs that are less sensitive to variations in the pressure drops across the nozzle [7].

6.0 SOUND MODULATION

In order to assess the capabilities of the STRATOJET to be amplitude-modulated, the response of the system to a controlled velocity modulation was investigated. We know that the amplitude of oscillations in the organ pipe vary with the jet velocity, or Mach number, as indicated on the examples of Figure 17. These curves show a very significant drop of the relative pressure oscillations in the pipe when the velocity is off the peak velocity. For example, for the optimum curve, $S_d \approx 0.30$, the amplitude of the relative pressure oscillations is reduced at least by a factor of four when the mean velocity deviates by plus or minus twenty-five percent from the peak. This shows the great capability of the STRATOJET to achieve large amplitude modulation with relatively low flow rate modulations. In fact, this is possible as long as the STRATOJET system is able to respond to the flow modulation, i.e., as long as the time response of the system is shorter than the modulation period. More precisely, the time response of the Organ Pipe STRATOJET is expected to be a fraction of the smaller of the two times: the main period of oscillation of the organ pipe and a time based on the thickness of the nozzle orifice lip and on the convection velocity of the generated ring vortices.

In order to investigate the capability of the STRATOJET to be modulated, a rotating disk which periodically partially interrupts the flow in the feed line (known as a chopper) was used to modulate the flow rate. The disk introduces a variable pressure loss in the system which periodically changes the flow rate. A sketch of the system concept is shown in Figure 18, and a picture is shown in Figure 19. The rotating disk which is off-centered from the feed pipe axis moves in a sealed box and partially

constraints the flow passage of the feed pipe. Therefore, the flow rate varies periodically with time, as does the pressure drop across the valve. The amplitude of modulation is controlled by the size and position of the disk, while the frequency of modulation is determined by the speed of rotation of the disk and the number of indentation or openings it contains (see Figure 18).

The feasibility study was conducted in the small visualization cell facility described in [3], and a preliminary test was run in the deep well of Hydronautics Ship Model Basin. The chopper was inserted in the feed line between the pump and the plenum preceding the organ pipe, and the acoustic characteristics of the system were investigated for various rotation speeds of the chopper. A transducer located at midlength of the organ pipe and a hydrophone positioned in the cell were used to monitor the oscillations. The system proved to work very satisfactorily. The pressure fluctuations due to the partial interruption of the flow were highly amplified, and the corresponding frequency of modulation was almost as energetic as the main STRATOJET frequency. Figures 20 and 21 show two examples of the frequency spectrum of the signal detected by the transducer at midlength of the organ pipe. In both cases, the main frequency of oscillation of the organ pipe was about 700 Hz. The frequency of interruption of the flow by the chopper was 180 Hz in the case of Figure 20, and was about 300 Hz in the case of Figure 21.

Figures 22 and 23 show the influence of flow modulation on the pressure fluctuations generated at midlength of the organ pipe. Two cases are considered. In Figure 22 the pressure drop across the nozzle is about 0.345 MPa (50 psi). This value corresponds to the lower end of the range of Mach numbers where

self oscillations of the STRATOJET are significant. However, the oscillations are relatively modest and do not exceed 6 percent in absence of modulations. Figure 22 shows that in this case the modulation of the flow rate entering the organ pipe modifies the root mean square value of the velocity fluctuations, $\bar{p}'$. The modulations seem to increase $\bar{p}'/\Delta P$ for all tested values of the cavitation number, σ, and of the modulation frequency. In addition, very significant amplifications are seen at the modulation frequencies of 200 and 300 Hz. A possible explanation for this observation is that these frequencies, being respectively the second and the first subharmonics of the Organ Pipe frequency ($\approx$600 Hz), have set up resonant oscillation in this Organ Pipe. This effect seems to be much more significant for the higher cavitation numbers where cavitation effects decay. The modification of $\bar{p}'/\Delta P$ with the flow modulation is much less apparent in Figure 23. In that case, the pressure drop across the nozzle is about 0.379 MPa (55 psi) and corresponds to the peak Mach number for the oscillations. An apparent saturation of the oscillations is seen and no influence of the modulation is observed. The nozzle is seen to have very strong oscillations between the values of sigma of 0.55 and 0.87 where the relative pressure fluctuations exceed 50 percent. A peak value of about 95 percent is achieved at a value of the cavitation number of 0.75.

A set of preliminary tests were conducted in the deep well of the Hydronautics Ship Model Basin using the 1.25 cm (0.5 in.) STRATOJET assembly described in the preceding section and the same chopper. The distance between the chopper and the nozzle was significantly greater than for the test conducted in the visualization cell and described above. This was imposed by the need to keep the chopper and its drive out of the water when the

nozzle was lowered into the well. This required a 15.24 m (50 ft)distance between the chopper and the nozzle. As a result, the amplitude of the modulation seemed to be significantly damped in the line. Figures 24 and 25 show two cases at peak pressure oscillation ($\Delta P \approx 0.427$ MPa (62 psi)). The chopper frequency was 240 Hz in Figure 24 and 330 Hz in Figure 25. The modulation frequency is seen in both figures in the hydrophone and transducer frequency spectra. It's level is, however, significantly lower than that of the main organ pipe frequency. Conceptually, there should be no major difficulties in improving this sytem given additional time and effort.

7.0 SOUND GENERATION ENHANCEMENT

The theoretical studies that we have conducted earlier concerning the collapse of a toroidal cavity [9 - 11] have shown the great importance of the vortex circulation Γ. Since the pressure drop at the ring vortex center is directly proportional to the intensity of circulation, Γ has to exceed a minimum value for cavitation to occur. Similarily, the higher Γ is the larger is the cavitation itensity at the vortex center. On the other hand, the theoretical results show that the intensity of the collapse is damped by a high value of the circulation. Therefore, a high value of Γ is needed for cavitation inception while a much lower value is desirable to achieve a strong collapse. This has prompted us to devise a means of modifying the circulation during the evolution of the phenomenon. By doing so, an intense circulation is initially achieved generating a strongly cavitating vortex ring. Later, during the collapse, the circulation is modified or interrupted using external means such as other vortices (opposed jets) or solid manipulators (solid enhancers), thus strengthening the collapse.

7.1 Opposing Jets

The first idea for circulation manipulation that we tested consisted of two opposing resonating jets. A new visualization facility was constructed and used for investigating the interaction between the rings generated by these jets.

The test chamber was a clear acrylic cylinder with aluminum end plates. The cylinder was 85.1 cm (33.5 in.) long and had a inner diameter of 21.6 cm (8.5 in.) in the middle 34.3 cm (13.5 in.) section and diameter of 17.8 cm (7 in.) at the end

portions. The axis of the cylinder was positioned horizontally and two STRATOJET nozzles penetrated the two sealed aluminum end plates and faced each other in the cell. The distance between the two nozzles could be easily changed. A small positive displacement pump served to pressurize the test cell. A centrifugal pump recirculated water from the test cell and discharged through flexible hoses and a tee junction into two plenums feeding one STRATOJET each. The flow through each nozzle was regulated by a discharge valve (see Figure 26). A transducer was located at midlength of each organ pipe and measured the pressure fluctuations in the resonant pipes. A hydrophone and/or a transducer were used to monitor the pressure oscillations or sound generated in the test chamber. Reflections on the test walls were undoubtedly important but were disregarded since relative sound pressure measurements, not absolute measurements, were sought.

The two organ pipes were 1.1 m (44 in.) long each. The two nozzles had shapes identical to those described in Section 3 and had 1.0 cm (0.4 in.) diameter orifices. The oscillation characteristics of each of the two STRATOJETs was the same as has been described earlier ([3] and Section 4) when the other jet was turned off. This is to be expected since the flow system sketched in Figure 26 becomes similar to that used earlier for single STRATOJET studies when one of the two valves, A or B, is closed. Ideally when valves A and B are opened equally the two nozzles behave symmetrically. Under ideal cavitating conditions two bubble rings issue from each nozzle and approach each other. When their distance is small enough both rings stretch (similar to a ring approaching a wall) and strongly interact. Since the two circulations are of opposite signs they cancel each other generating a strong vortical cavity collapse. Practically, this

ideal situation is not easily achievable. Any small asymmetry in either the geometric configuration (e.g., the two jet centerlines are not exactly aligned) or the hydrodynamic conditions (e.g., the two jet instantaneous velocities are not equal) prevents the merger of the two rings as described above. As seen with high speed movies these asymmetries introduce either an inclination of the stretching plane and/or a displacement of the stagnation point from the mid-distance between the two nozzles closer to one of these nozzles. Figures 27 and 28 show two sequences from high speed motion pictures of the phenomena. In both cases asymmetry has prevented an energetic vortex ring merger. Vortex rings approaching each other are not of equal size in Figure 27 probably due to a phasing between the ring vortex emission of each nozzle. In addition a slight misalignment has generated a plane of spreading and stretching of the rings non-perpendicular to the jet axis. A probable small difference in the jet velocities has moved the stagnation point towards one of the nozzles. As can be guessed from these pictures, rings from the two STRATOJETs do not merge and collapse simultaneously and therefore the required collapse enhancement is not achieved. Figure 28 shows a case where the only asymmetry is the jet axes misalignment. In this case a stronger ring cavity implosion is achieved.

Figure 29 gives an example of the pressure fluctuations signals detected at different locations. Simultaneously shown are the pressure signals detected by the transducers located at midlength of each of the organ pipes and the sound measurement obtained by a hydrophone located in the midplane between the two nozzles. Almost pure sinusoidal pressure fluctuations are seen by the two transducers. The frequency of these fluctuations appears to be the same for both STRATOJETs and corresponds to the

organ pipe natural frequency ($\simeq$ 600 Hz). The amplitudes of the two signals are also very comparable. However, a close look at the two transducer signals shows a phasing between the pressure fluctations. This phasing is intimately related to the asymmetries seen in the pictures in Figures 27 and 28. The signals of the hydrophone are distinguishable from the transducer signals by their content of high frequency oscillations which are directly related to their detection of the cavitation events.

A comparison between the rms amplitudes of the hydrophone signals generated by an isolated STRATOJET and two opposing STRATOJETs does not produce very encouraging results. As shown in the following table which presents a characteristic example of the results obtained both off-peak and at-peak resonance, the pressure generated by the dual jets remains of the same order as twice the noise generated by a single jet. Since the energy consumption is twice as large there is no gain in using the opposing jet for noise enhancement. We repeat again that this is mainly due to the difficulty in obtaining a perfect alignment, symmetry, and tuning of the two jets. This concept was abandoned in favor of the enhancers described below.

ΔP psi	P_a psi	X* in.	$\bar{p}'^{**}_p$ psi	$\bar{p}'^{***}_h$ psi	Configuration
30	30	2	3.1	0.075	Isolated 1
30	30	2	3.5	0.100	Isolated 2
30	30	2	5.75, 4.0	0.225	Dual
50	50	2	81	0.325	Isolated 1
50	50	2	80	0.275	Isolated 2
50	50	2	75, 75	0.535	Dual
50	50	10	85	0.20	Isolated 1
50	50	10	87.5	0.375	Isolated 2
50	50	10	83.25, 83.25	0.450	Dual

* Distance between nozzles
** rms pressures detected by a transducer located at midlength of the Organ Pipe.
*** rms pressures detected by a hydrophone at mid-distance between the nozzles.

7.2 Solid Enhancers

Another way to enhance the intensity of bubble ring collapse by manipulating the circulation of the ring vortices is to induce their interaction with solid boundaries. The simplest concept which proved to be effective very early in our studies was the use of an impacted solid flat plate. A bubble collapsing while approaching a solid wall behaves similar to two bubbles approaching each other [11, 12]. Using the same principle of images, a structured jet impacting a solid wall is similar to two perfectly identical jets opposing each other. Therefore, the generated noise is expected to be greater than with an isolated jet. As compared with actual dual opposing jets the jet impacting on a solid wall has the advantage of imposing a perfect symmetry. This avoids the problems described in the preceding section such as phasing or difference in size between the interacting rings. On the other hand, the eventuality of merging of the two colliding rings is then nonexistent. Instead, a ring and its image approach each other exponentially, and their later behavior is controlled by viscosity near the solid wall. The intensity of the collapse is further enhanced by a nonsymmetrical bubble ring implosion [11]. Therefore, an intensification of the emitted noise by a factor greater than two is expected.

The first set of tests conducted in the visualization cell described earlier [3] proved this to be true. As can be seen from Figure 30, enhancement values as high as 4.5 were observed when the standoff distance between the jet and the plate was optimized. However, later repetitions of these tests, have shown lower enhancement values obtained from average values of several tests. Figure 31 shows results obtained from averaging data

obtained for repeated tests at various dates and hours. Variations can only be imputed to unknown factors or the water quality (air content, etc.) in the test facility. At peak performance ($\Delta P \approx 0.483$ MPa (70 psi)) the flat plate enhancement factor is close to 2.2 (≈ 6.8 db).

Following this initial success of the noise enhancement of self resonating cavitating jets several other ideas were investigated. All these tests were conducted in the small visualization cell and focused primarily on a feasibility investigation study. The most significant tests involved the following configurations on which the jet was impacted:

a. Solid flat plate perpendicular to the jet axis,
b. Solid plate with perpendicular ribs,
c. Solid flat plate with holes,
d. Splitter plate cutting the jet,
e. Ring hollow cylinder with the same axis as the jet,
f. Helmholtz chamber at the nozzle exit, and
g. Multiple plates with orifices centered on the jet axis.

Below, we will briefly discuss the most promising configurations.

The basic idea behind inserting flat obstacles which are parallel to the jet axis in the ring vortex path, was to attempt to locally destroy the vortex circulation in order to enhance the collapse intensity. This objective was intended in configurations b and d. However, no significant improvement relative to the flat plate case was found for the limited set of configurations tested (see Figures 32 through 34). Configuration d also turned out to be not too promising. In the first case the ring

vortex trajectories were modified by the obstacle plates and thus avoided destruction. In the second case, the vortex rings were manipulated only locally and no significant improvement ensued.

Figure 32 shows the results obtained with circular shaped riblets ("O" rings) located on a flat plate and centered below the impacting STRATOJET. Various diameter riblets are shown. All were 0.64 cm (0.25 in.) thick and 0.64 cm (0.25 in.) high (the dimensions were chosen arbitrarily). In most, if not all cases, the noise generated fell below that obtained with a flat plate. The results are, however, very much dependent on the size of the ring and the plate-nozzle distance. Figure 32 shows also, an attempt to interfere with the ring vortices using depressions instead of riblets. Centered on two circular lines of diameters 1.59 cm (0.625 in.) and 2.22 cm (0.875 in.) a set of holes 0.318 cm (1/8 in.) deep were drilled. The holes had a diameter of 0.159 cm (1/16 in.) and a separation distance between each other of 0.318 cm (1/8 in.). Results close to the flat plate were obtained for a standoff distance of 1.25 cm (0.5 in.). However, a loss of efficiency was observed for X ≈ 0.635 cm (0.25 in.).

Figure 33 shows results of a non-successful attempt to improve on the circular riblet configuration by using two perpendicular plates 0.318 cm (1/8 in.) wide and 0.635 cm (1/4 in.) high positioned as a cross, centered under the jet axis. This figure compares the cases where the cross was alone and where it was positioned inside the circular riblets.

Another more successful attempt to enhance the noise generation of the jet was made by using the "bird whistle" principle. Vortex rings impacting at the hole boundary send upstream a pressure signal which upon reaching the nozzle orifice enhances

the formation of exiting vortices if the timing is well correlated. A circular hole was drilled in the flat plate and the effect of the standoff distance between the nozzle and the plate, X, was investigated. Only a few diameters of the hole were investigated. Figure 34 shows the results obtained with a 1.25 cm (0.5 in.) diameter hole. Depending on the distance X, significant enhancement can be achieved. For X ≈ 0.635 cm (0.25 in.) an amplification factor close to 2.5 (≈ 8 db) is observed. The relative position between the jet axis and the hole center was also investigated. The hoped for additional increase of noise emission due to ring disruption and to secondary cavitation at the hole did not materialize, and the noise generated was always close to or below that of a simple flat plate.

A configuration which also showed some promise consisted of a hollow cylinder, or a circular wide band positioned in front of the jet. The axis of the cylinder coincided with that of the jet, and it's radius corresponded to that of the axisymmetric jet shear layer. Ring vortices were forced to collapse on the cylinder walls. Figure 35 shows a set of tests conducted with a succesful enhancer. The inside diameter of the cylinder was 1.04 cm (0.41 in.), its outside diameter was 1.25 cm (0.5 in.) and its length was 0.533 cm (0.21 in.). The noise generated at approximately 8.9 cm (3.5 in.) and 90° from the nozzle axis is shown for several nozzle-enhancer distances, X. A strong dependence on X can be seen indicating the probable presence of several preferred values if a continuous change in X is investigated. A probable feedback mechanism between rings imploding on the cylinder and the nozzle exists. In the set of tests shown in Figure 31, a distance of 2.54 cm (1 in.) seems to be the most effective of those tested, generating more than twice (≈ 7 db) as much noise as the isolated jet case. Time did not allow for a more thorough

investigation of the cylindrical enhancer. For instance, an optimization of the cylinder length, diameter and band width could increase significantly the amplification factor.

The next attempt to amplify the noise generated by a STRATOJET self resonating cavitating jet was based on dual orifice resonators or hole-tone oscillators. Given that the organ pipe STRATOJET was generating enough oscillations to produce strong bubble rings, the objective of the enhancer was to extend the presence of rings further in front of the nozzle and, in addition, to enhance their collapse. The principle of operation of the dual orifice oscillators is similar to the bird whistle principle described above. A ring vortex emitted from Orifice A (Figure 36) traverses downstream at it own translation velocity and sends a pressure signal when it reaches Orifice B. This signal traverses upstream at sonic speed and if it reaches Orifice A at the time where another vortex is in the formation stage, it triggers a stronger circulation. This feed back mechanism generates strong vortices between the two orifice plates. Implosion is enhanced by the presence of the two plates. Several factors influence the efficiency of such an enhancer, namely the hole diameters d_1 and d_2 and the distances X_1 and X_2 relative to the jet diameter d_j (see Figure 36). As we will see below this efficiency can be further improved by using an additional impacted solid flat plate positioned at a distance X_3.

Figure 37 shows the variations of the pressure fluctuations in the cell with the pressure drop across the nozzle as measured by a hydrophone located 8.9 cm (3.5 in.) from the jet axis and 1.25 cm (0.5 in.) above the nozzle exit plan. Baselines are given in this figure for a flat plate enhancer positioned 0.635

cm and 1.25 cm (1/4 and 1/2 in.) from the nozzle. The measured values are also compared with an isolated STRATOJET. In the cases studied, the configuration in which the two orifices had a diameter of 1.25 cm (0.5 in.) and were located at the distances 0.635 cm and 2.22 cm (1/4 in. and 7/8 in.) from the nozzle showed the greatest amplification. The generated noise attained about 2.8 times that achieved with an isolated STRATOJET. This is about 9 db more than the isolated nozzle.

Since an impacted flat plate showed a very signficiant enhancement with an isolated STRATOJET we thought to combine it with this "best" dual orifice enhancer. A flat plate was positioned in front of the dual orifice STRATOJET configuration at a distance X_3 and its influence was investigated. Figures 38 and 39 show some pictures of the ring vortices generated in the STRATOJET dual orifice configuration. Very fat vortices are seen when the pressure oscillations are very strong. Figure 40 shows the influence of the distance X_3 of the flat plate from the nozzle. An important amplification can be seen when the pressure drop across the nozzle, ΔP, is about 0.414 MPa (60 psi). The amplification factor achieved is about 4 ($\simeq$ 12 db) when X_3 is about 6.35 cm (2.5 in.). Figure 41 confirms this fact for various diameter holes of the dual orifices. The enhancer with 1.43 cm (9/16 in.) diameter holes achieves an amplification factor of 4.5 ($\simeq$ 13 db).

8.0 CONCLUSIONS

Noise generating properties of self-resonating cavitating jets, known as STRATOJETs, have been investigated and described. These jets organize into large coherent structures without the use of any external means or energy source. The interactions between the jet shear layer pressure fluctuations and the properly shaped nozzle exit cause feedback to an Organ Pipe tube feeding the nozzle. This Organ Pipe acts as an amplifier when its frequency matches the submerged jet natural oscillation frequency. The tests conducted have shown that the efficiency of the STRATOJET is at least two orders of magnitude higher than a conventional cavitating non-excited jet. The emitted signal decreases as the inverse of the distance from the nozzle. A very discrete frequency can be obtained with the system and can be controlled by changing the STRATOJET geometry. Scaling effects have been investigated, but isolating the various effects has proven to be difficult. The influence of cavitation, nozzle diameter, organ pipe length and pressure drop across the nozzle was studied. The nozzle shape investigated is seen to form a STRATOJET which is a strong noise generator only in a range of values of the cavitation number or the pressure drop across the nozzle. Using an external source of energy, a chopper was utilized to modulate the flow to the STRATOJET. The generated noise was seen to contain both the main oscillation frequency as well as the frequency of modulation generated by the chopper. These tests are preliminary in nature and need to be repeated in the large test facility.

In an effort to enhance further the STRATOJET generated sound, opposing jets and solid enhancers were used. In these schemes manipulation of the vortex circulation was sought. While

opposing jets did not readily produce the expected reuslts, several solid enhancers were discovered. Amplification factors as high as six were found with these enhancers without any additional source of energy. The simplest noise enhancer consists of a simple flat plate positioned in front of the nozzle. These very encouraging results were obtained in the small visualization cell. It would be very desirable to confirm these results in a large facility.

The results of this study strongly suggest that a system based on a STRATOJET, possibly with some form of enhancers, would make a very effective noise generation source. Additional investigation with large scales would enable confirmation of these promising tentative results and provide better definition of the details and sensitivities of such a system.

9.0 REFERENCES

1. Johnson, Jr., V. E., Chahine, G. L., Lindenmuth, W. T., Conn, A. F., Frederick, G. S., and Giacchino, Jr., G. J., "Cavitating and structured Jets for Mechanical Bits to Increase Drilling Rate," ASME Journal of Energy Resources Technology, Vol. 106, pp. 282-294, June 1984.

2. Chahine, G. L., Johnson, Jr., V. E., Lindenmuth, W. T., and Frederick, G. S., "Noise Generated by a Self-Resonating Cavitating Jet," ASME Cavitation and Multiphase Flow Forum 1984, New Orleans, Louisiana, pp. 26-30, February 1984.

3. Chahine, G. L., Johnson, Jr., V. E., Lindenmuth, W. T., and Frederick, G. S., "The Use of Self-Resonating Cavitating Water Jets for Underwater Sound Generation," Tracor Hydronautics Technical Report 83005-1, November 1983. Also Journal of the Acoustical Society of America, 77, (1), pp. 113-126, January 1985.

4. Chahine, G. L. and Johnson, Jr., V. E., "Mechanics and Applications of Self-Resonating Cavitating Jets," ASME International Symposium on Jets and Cavities, WAM, Miami, Florida, November 1985.

5. Chahine, G. L., Genoux, Ph. F., Johnson, Jr., V. E., and Frederick, G. S., "Analytical and Experimental Study of the Acoustics and the Flow Field Characteristics of Cavitating Self-Resonating Water Jets" Tracor Hydronautics Technical Report 82009-1, May 1984; Sandia Report SAND84-7142.

6. Jorgensen, D. W., "Noise from Cavitating Submerged Jets," Journal of the Acoustical Society of America, 33, pp. 1334-1338, 1961.

7. Chahine, G. L., Liu, H. L., Johnson, Jr., V. E., and Frederick, G. S., "Development of a STRATOJET Nozzle for Optimum Resonance in Drilling Mud," Tracor Hydronautics Technical Report 84004-1, July 1984.

8. Chahine, G. L., Sirian, C. R., and Watson, R. E., "Application of Oscillating Jets to Improved PDC Bits," Tracor Hydronautics Technical Report 84006-1, August 1984.

9. Chahine, G. L. and Genoux, Ph. F., "Collapse of a Cavitating Vortex Ring," Journal of Fluids Engineering, Vol. 105, pp. 400-405, December 1983.

10. Genoux, Ph. F. and Chahine, G. L., "Collapse of a Toroidal Bubble Near a Solid Wall," ASME Cavitation and Multiphase Flow Forum, New Orleans, LA, pp. 69-72, February 1984.

11. Chahine, G. L., Genoux, Ph. F., and Liu, H. L., "Flow Visualization and Numerical Simulation of Cavitatin Self-Oscillating Jets," 7th International Symposium on Jet Cutting Technology, Ottawa, Canada, June 1984.

12. Chahine, G. L. and Bovis, A. G., "Pressure Field Generated by Nonspherical Bubble Collapse," Journal of Fluids Engineering, Vol. 105, No. 3, pp. 356-364, September 1983.

Table 1

STRATOJET Tests Ran in the Deep Well of the HSMB.
Chronologic Order Log

No.	d_{in}	D_{in}	e_{in}	L_{in}	$P_{a_{psi}}$	ΔP_{psi}	r_{in}	θ_{deg}	X_{in}	Remark
1	0.4	1.0	0.2	44	17	Var.	12	20	-	Free Jet
2	0.4	1.0	0.2	44	Var.	40	12	20	-	"
3	0.4	1.0	0.2	44	Var.	50	12	20	-	"
4	0.4	1.0	0.2	44	Var.	100	12	20	-	"
5	0.4	1.0	0.2	44	17	52	Var.	18	-	"
6	0.4	1.0	0.2	22	Var.	50	12	20	-	"
7	0.2	1.0	0.1	22	17	Var.	5.5	90	-	"
8	0.2	1.0	0.1	22	Var.	24	5.5	33	-	"
9	0.2	1.0	0.1	22	Var.	32	5.5	33	-	"
10	0.2	1.0	0.1	22	16.7	26	Var.	30	-	"
11	0.6	1.0	0.3	44	30	Var.	-	-	-	"
12	0.6	1.0	0.275	44	30	Var.	-	-	-	"
13	0.6	1.0	0.25	44	30	Var.	12	20	-	"
14	0.6	1.0	0.25	44	Var.	73	12	20	-	"
15	0.6	1.0	0.25	44	Var.	65	12	20	-	"
16	0.6	1.0	0.25	44	27.7	60	Var.	45	-	"
17	0.5	1.0	0.25	44	30	Var.	-	-	-	"
18	0.5	1.0	0.25	44	Var.	62	12	20	-	"
19	0.5	1.0	0.25	44	28	62	Var.	45	-	"
20	0.5	1.0	0.25	44	30	62	-	-	-	With Chopper
21	0.203	0.485	0.107	22	17	Var.	14	45	-	Free Jet
22	0.203	0.485	0.107	22	Var.	34	14	45	-	"
23	0.203	0.485	0.107	22	19	34	Var.	45	-	"
24	0.203	0.485	0.107	22	17	34	Var.	45	-	"
25	0.292	0.655	0.165	33	Var.	53	14	45	-	"
26	0.292	0.655	0.165	33	17	53	Var.	45	-	"
27	0.292	0.655	0.165	33	17	Var.	14	45	-	"
28	0.4	1.0	0.185	44	Var.	95	12	20	0.5	With Enhancer
29	0.4	1.0	0.185	44	Var.	67	12	20	0.5	"
30	0.4	1.0	0.185	44	17	96	Var.	20	0.5	"
31	0.4	1.0	0.185	44	17	Var.	36	20	0.5	"
32	0.4	1.0	0.185	44	17	32	Var.	20	0.125	"
33	0.4	1.0	0.185	44	17	06	Var.	20	-	Free Jet
34	0.4	1.0	0.185	44	17	32	Var.	20	-	"
35	0.4	1.0	0.185	44	17	32	Var.	20	0.25	With Enhancer
36	0.4	1.0	0.185	44	17	60	Var.	20	0.25	"
37	0.4	1.0	0.185	44	17	34	Var.	20	0.50	"
38	0.4	1.0	0.185	44	Var.	32	12	20	-	Free Jet
39	0.4	1.0	0.185	44	Var.	21	12	20	-	"

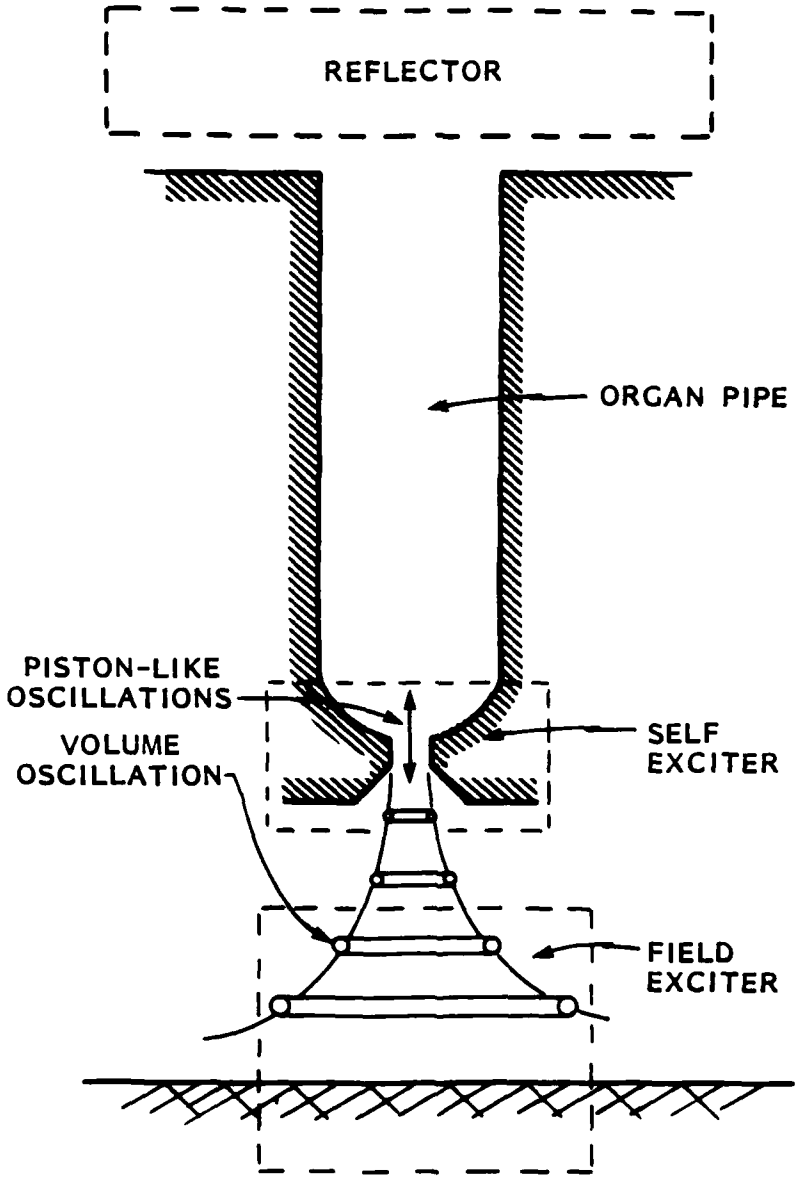

FIGURE 1 - STRATOJET-NOISE GENERATOR. SCHEMATIC OF OPERATION

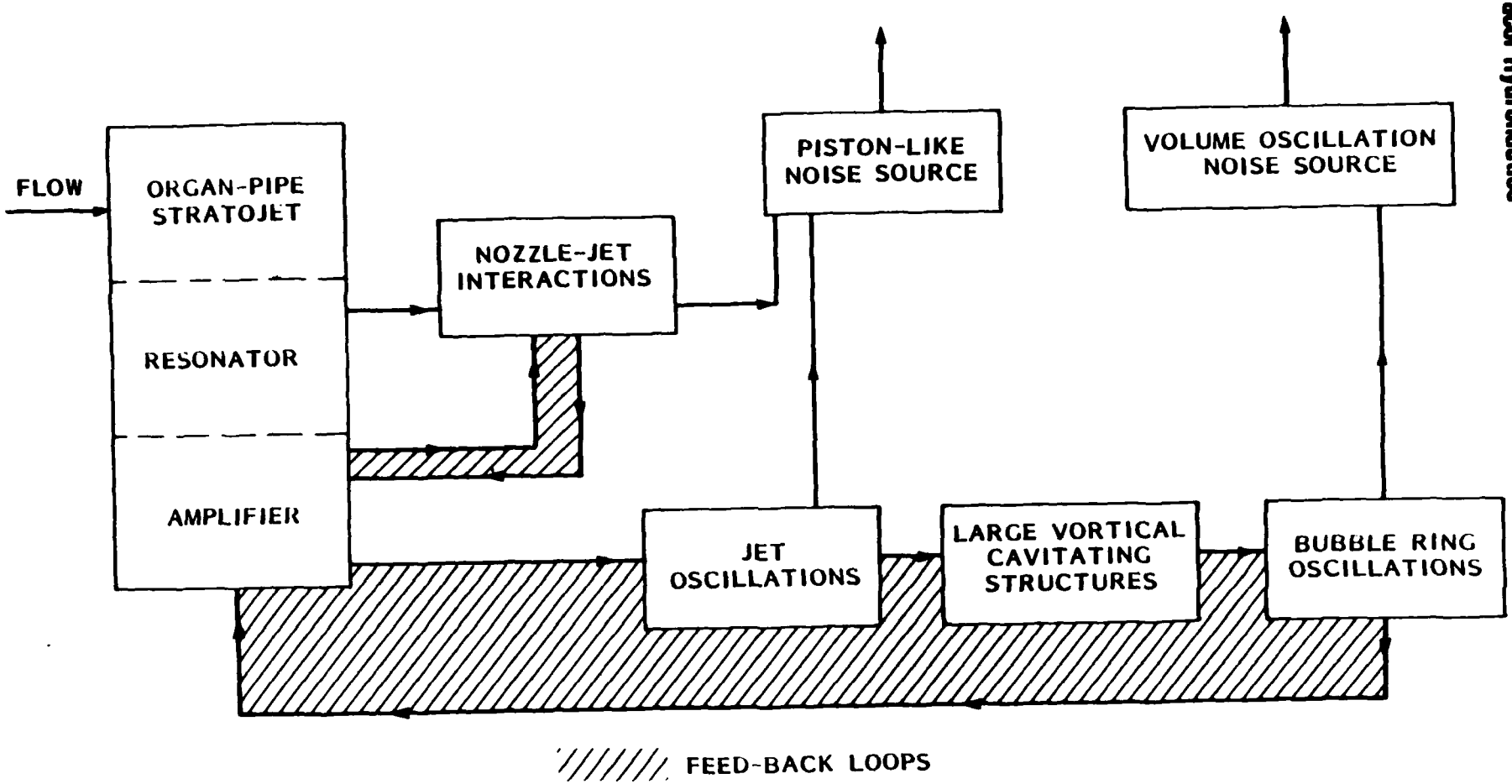

FIGURE 2 - DIAGRAM OF FEED-BACK MECHANISMS AND HYDRO-ACOUSTIC NOISE GENERATION OF AN ORGAN-PIPE STRATOJET

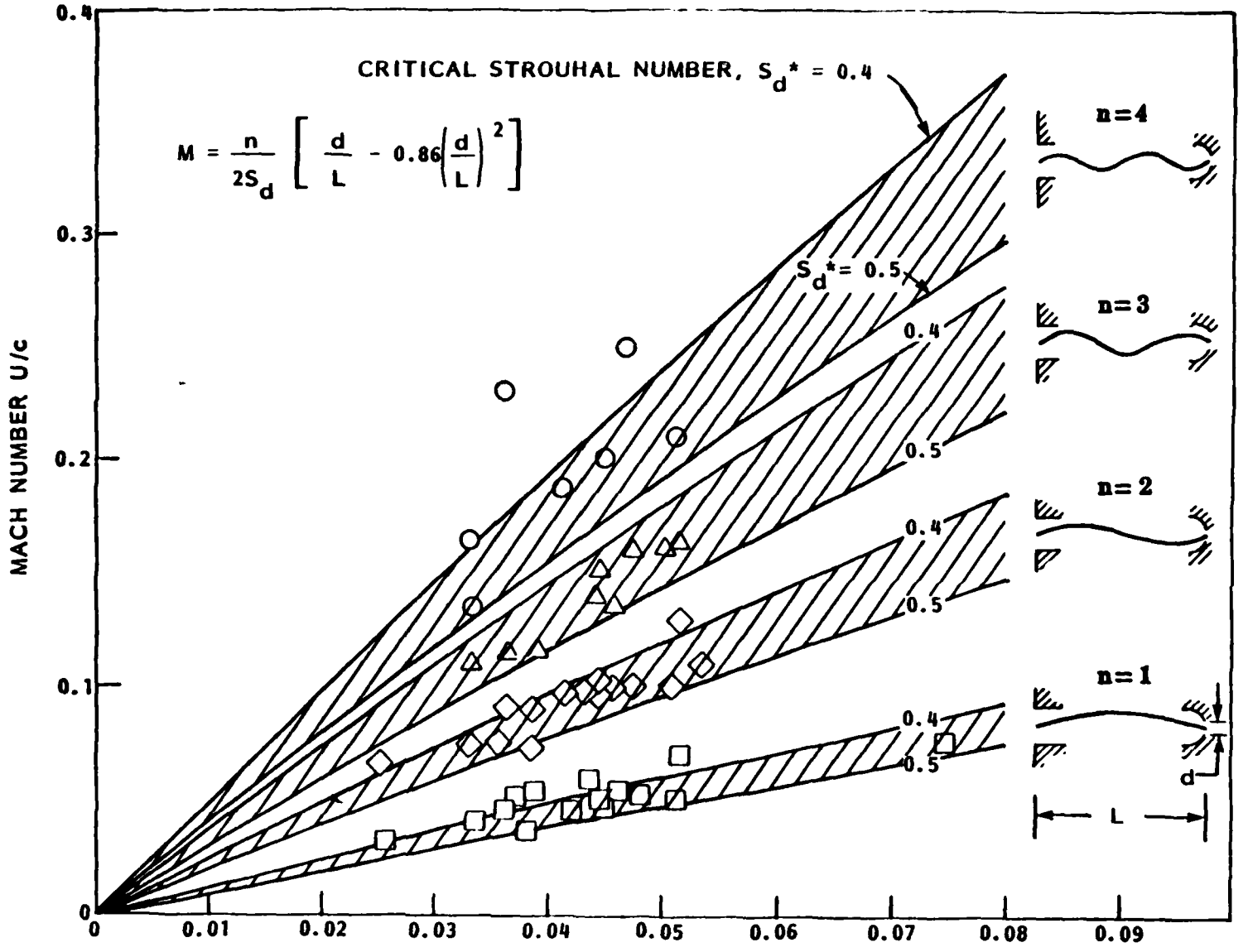

FIGURE 3 - CORRELATION OF OPTIMUM MACH NUMBER AND ORGAN-PIPE STRATOJET GEOMETRY

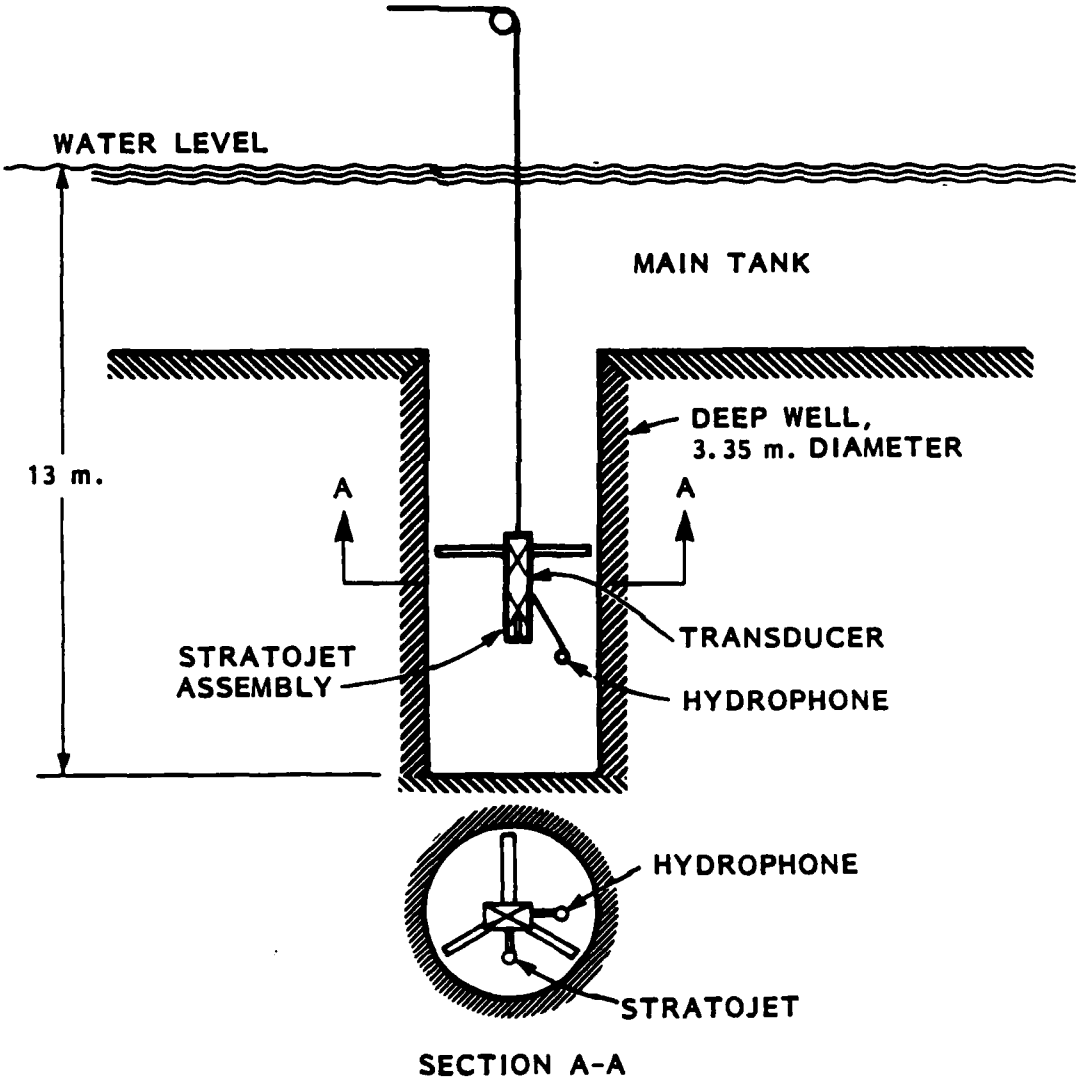

FIGURE 4 - SCHEMATIC OF SOUND MEASURING TESTS IN DEEP WELL OF TRACOR HYDRONAUTICS SHIP MODEL BASIN

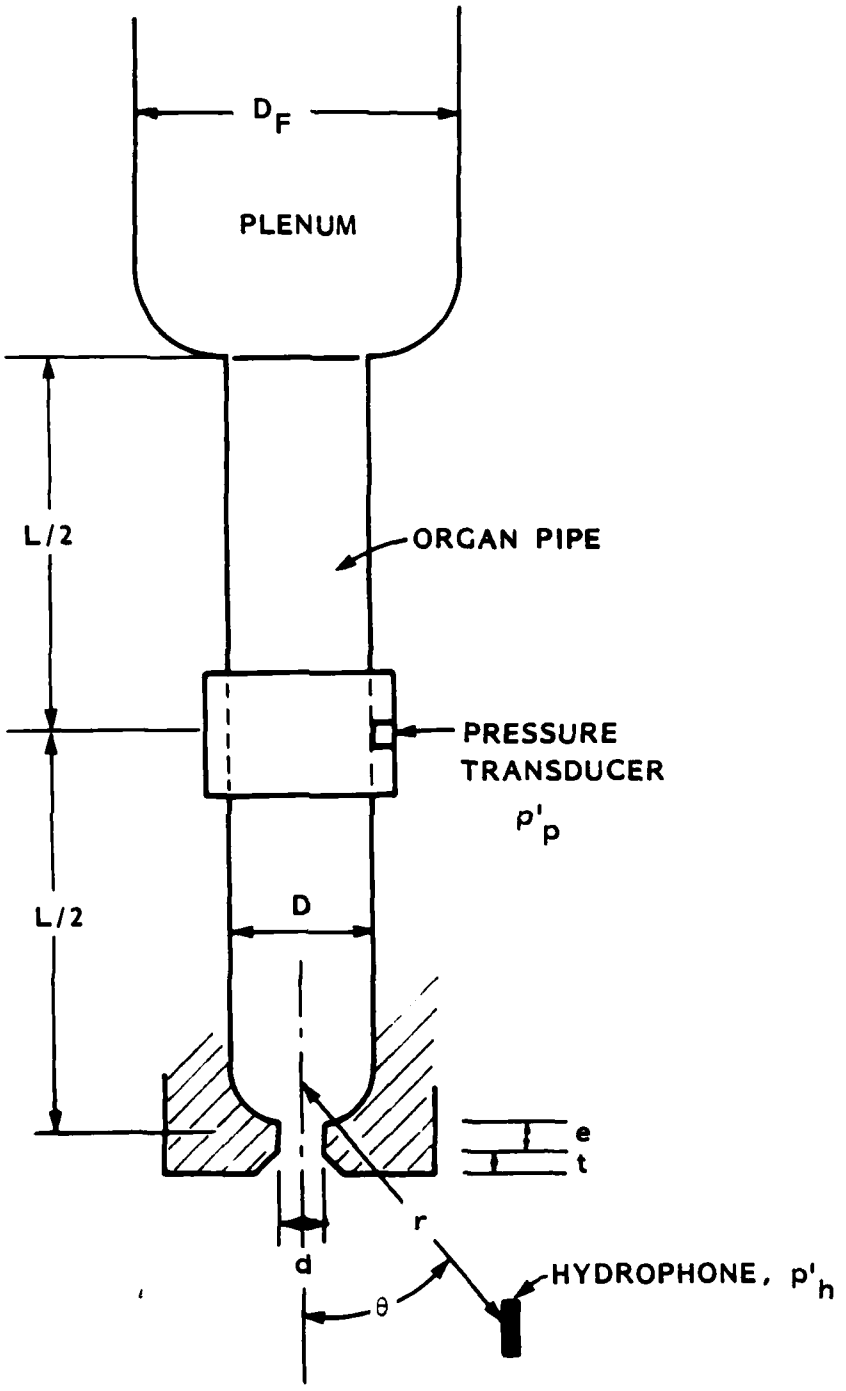

FIGURE 5 - EXPERIMENTAL SET-UP FOR NOISE MEASUREMENTS

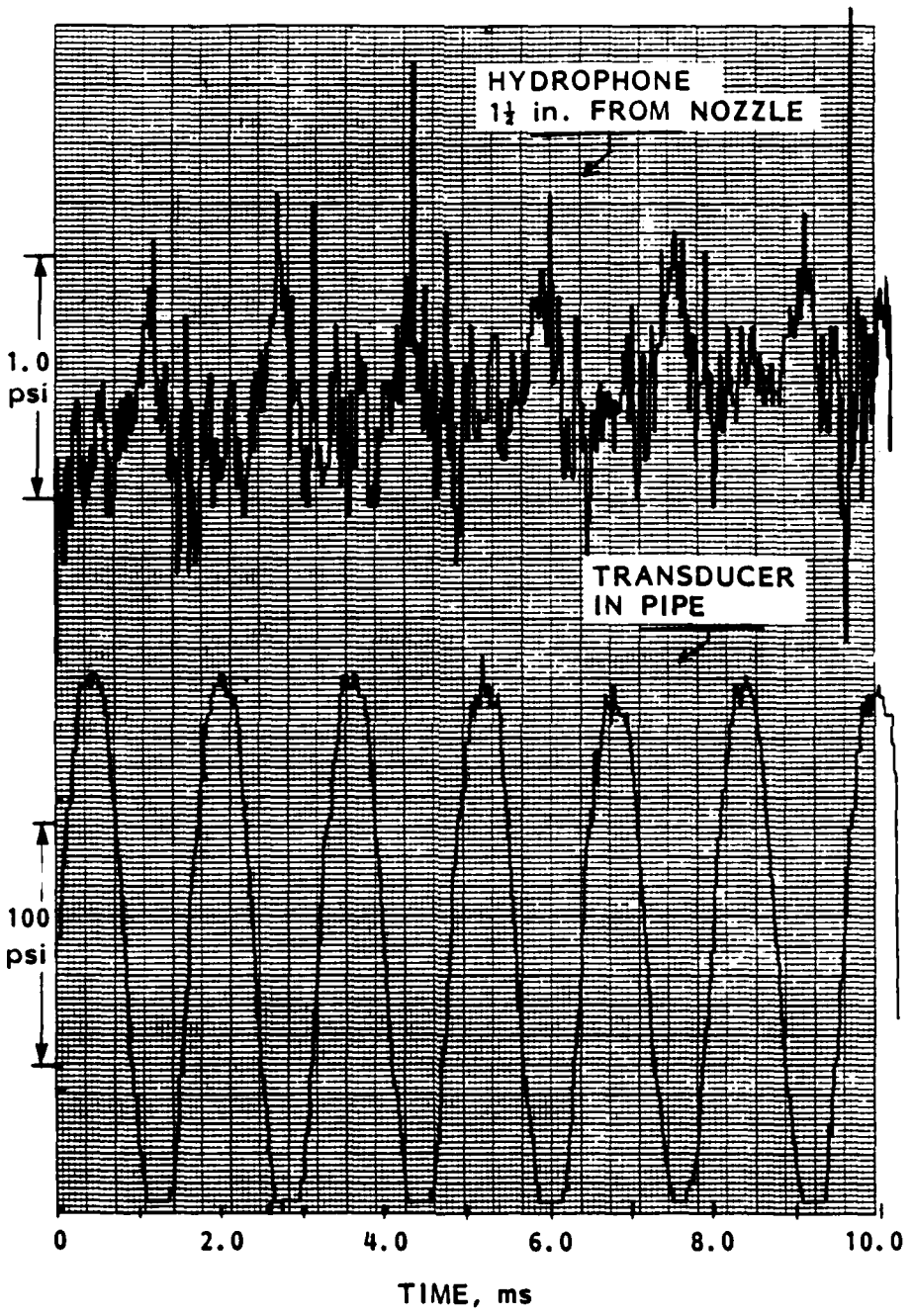

FIGURE 6 - COMPARISON OF RAW PRESSURE OSCILLATIONS SIGNALS IN PIPE AND IN CELL, (Δp = 50 psi, P_a = 50 psi)

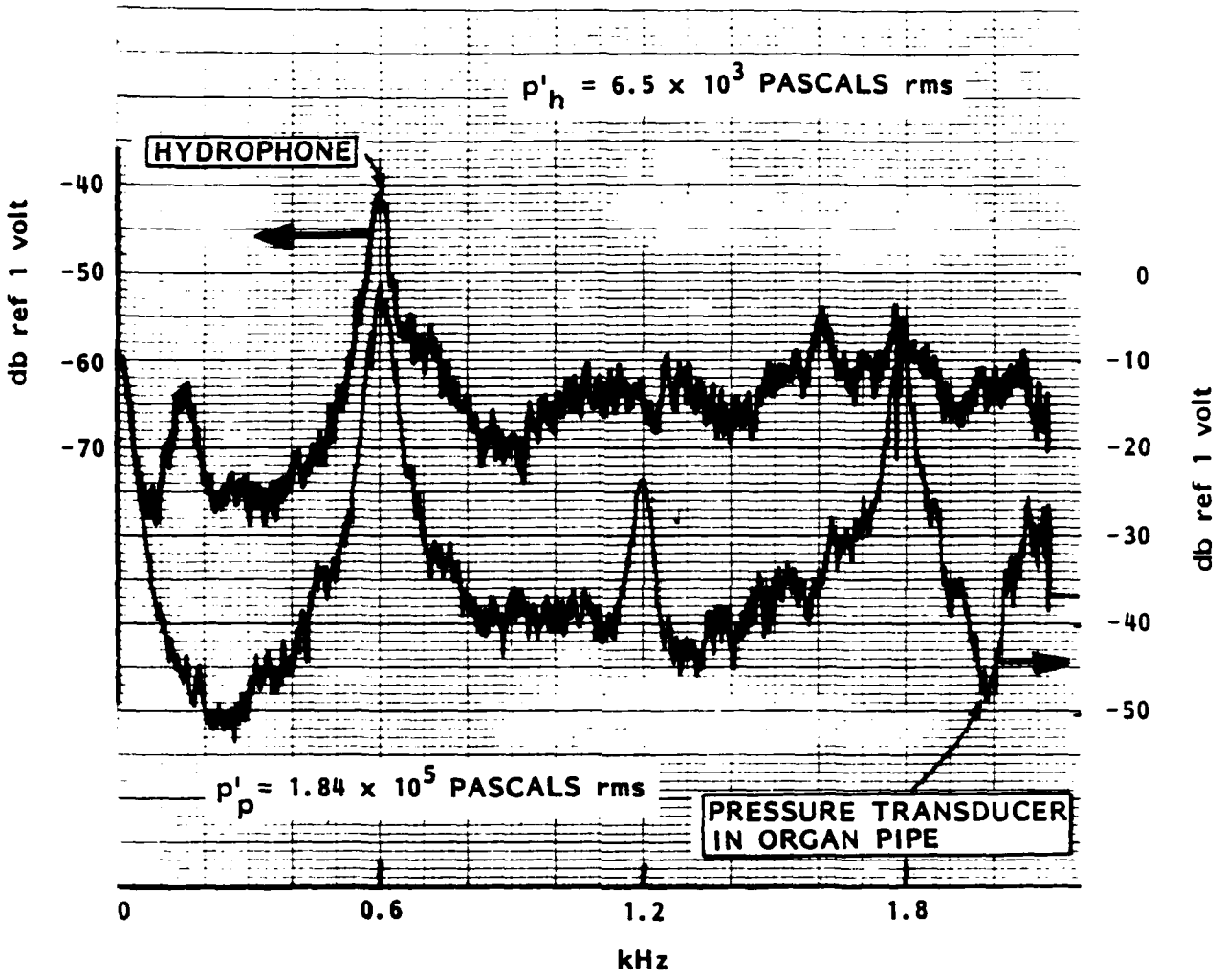

FIGURE 7 - FREQUENCY SPECTRUM OF PRESSURE FLUCTUATIONS IN PIPE AND OF ACOUSTIC PRESSURES AT $r = 0.92$ m, $\theta = 18°$, HYDROPHONE 3.4×10^4 PASCALS/VOLT, TRANSDUCER 1.4×10^5 PASCALS/VOLTS, $d = 1$ cm, $\Delta P \sim 0.35$ MPa

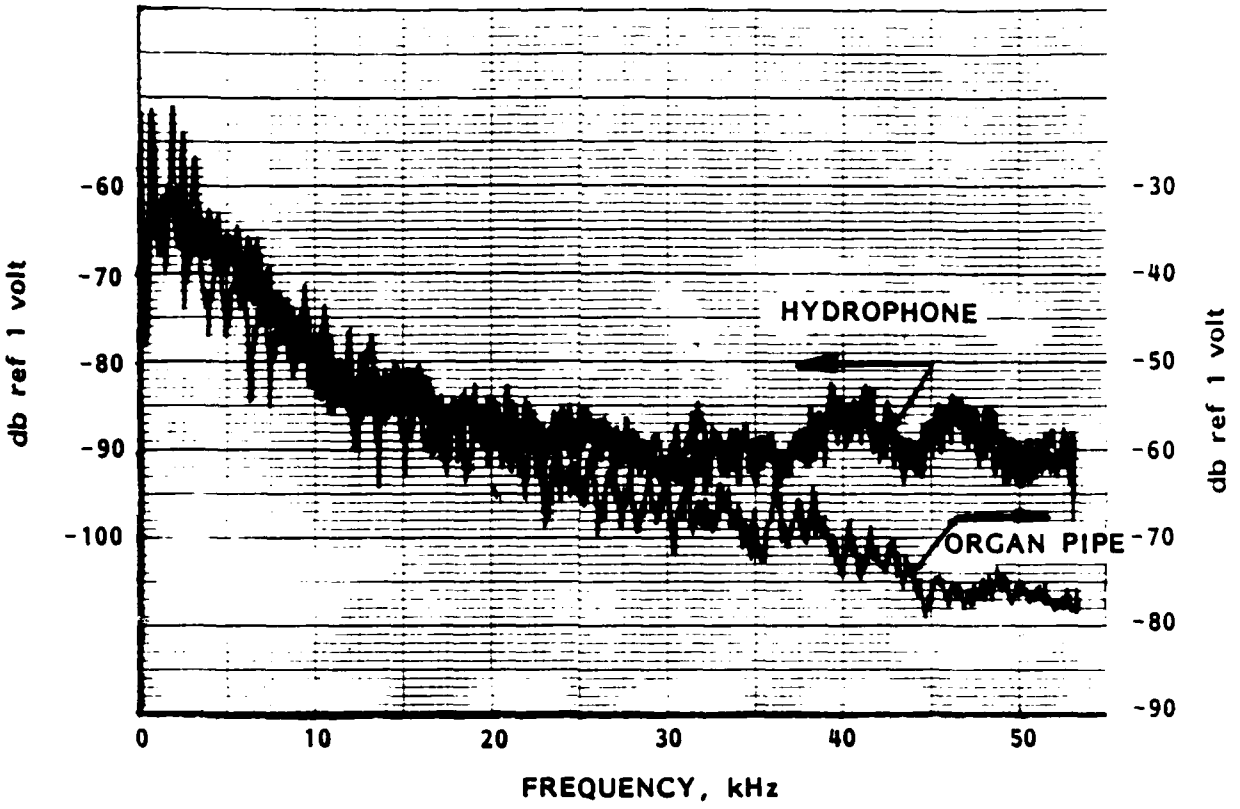

FIGURE 8 - FREQUENCY SPECTRUM OF PRESSURE FLUCTUATIONS IN PIPE AND OF ACOUSTIC PRESSURES AT r = 0.92 m, θ = 18°, HYDROPHONE: 1 volt = 3.4×10^4 PASCALS. TRANSDUCER: 1 volt = 1.4×10^5 PASCALS, d = 1 cm, $\Delta P \sim 0.35$ MPa

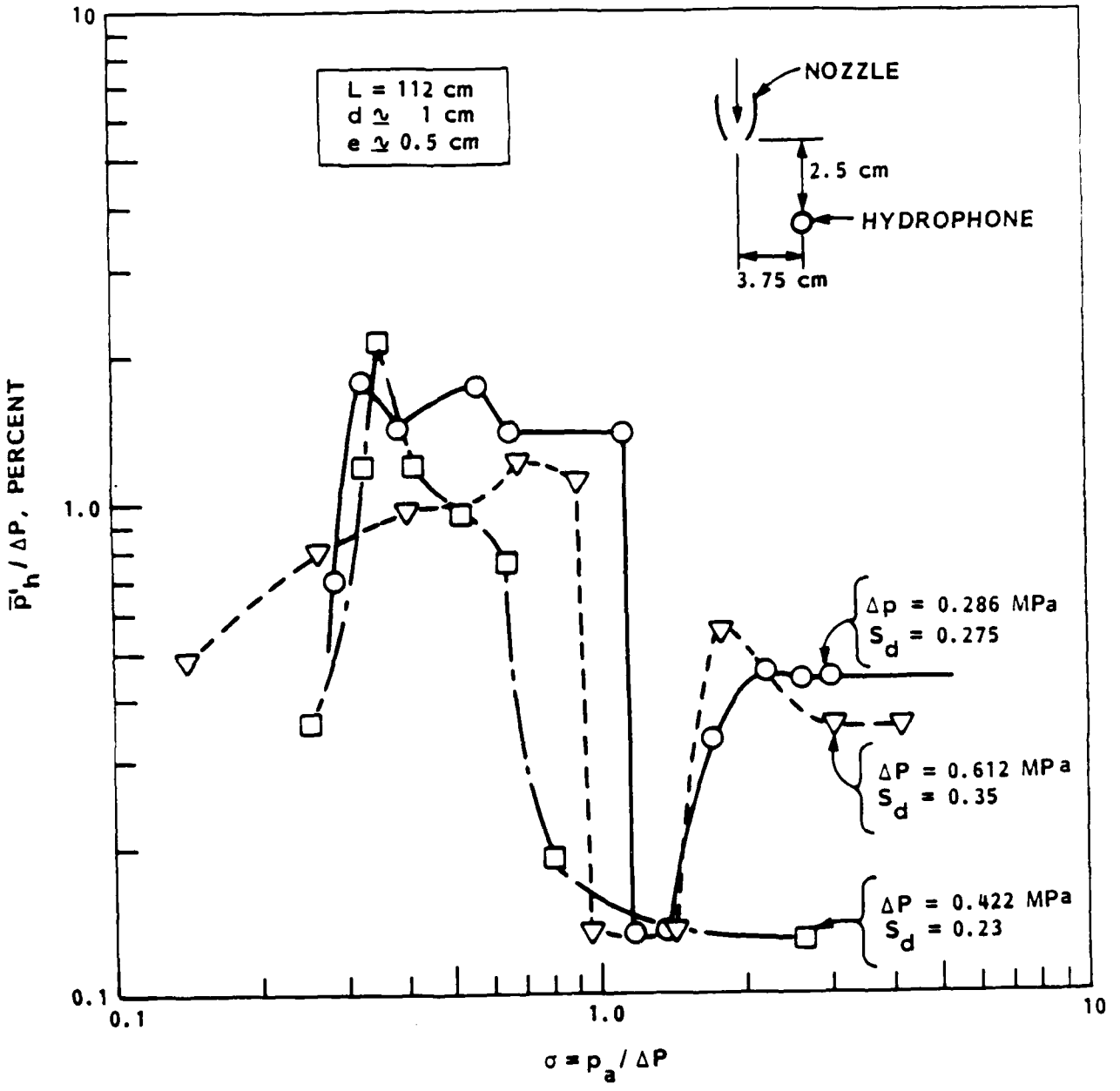

FIGURE 9 - RELATIVE FIELD PRESSURE OSCILLATIONS DUE TO A STRATOJET DETECTED BY A HYDROPHONE IN THE SMALL TEST LOOP.

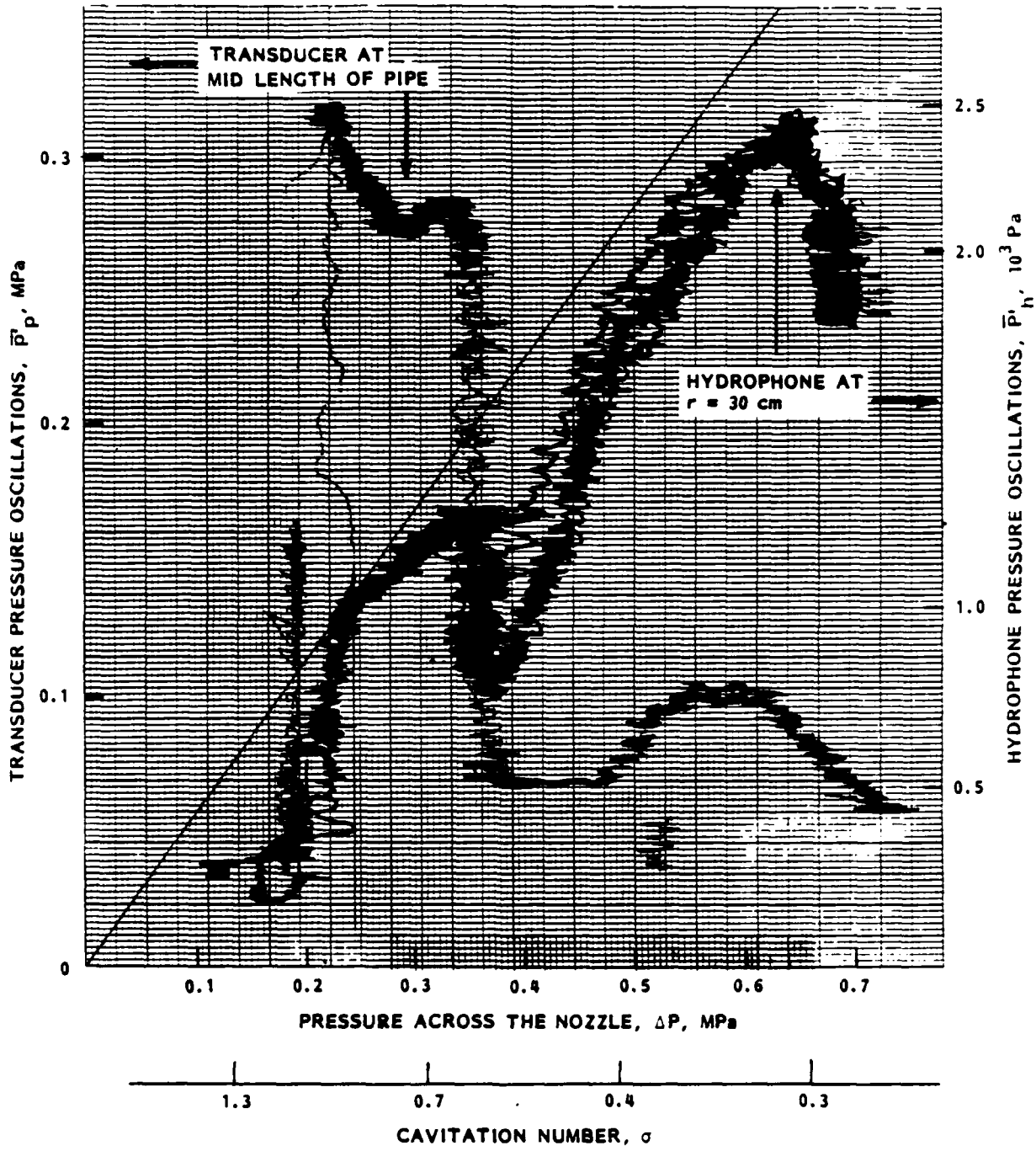

FIGURE 10 - VARIATION OF PRESSURE OSCILLATIONS AT TRANSDUCER AND HYDROPHONE LOCATIONS VERSUS THE JET VELOCITY AT FIXED JET SUBMERGENCE H ≈ 1.6 m

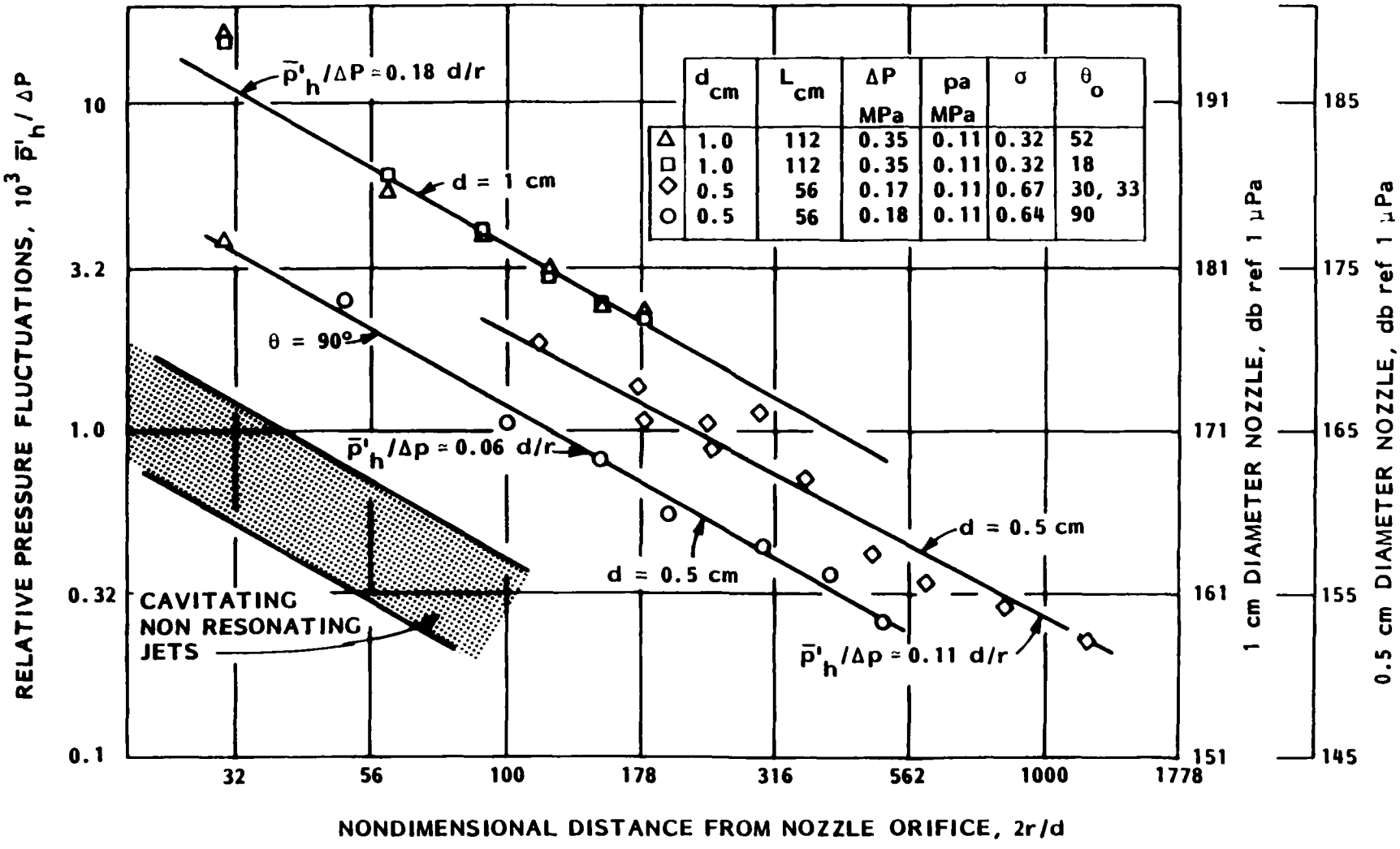

	d_{cm}	L_{cm}	ΔP MPa	pa MPa	σ	θ_o
△	1.0	112	0.35	0.11	0.32	52
□	1.0	112	0.35	0.11	0.32	18
◇	0.5	56	0.17	0.11	0.67	30, 33
○	0.5	56	0.18	0.11	0.64	90

FIGURE 11- ATTENUATION OF THE RMS VALUE OF THE PRESSURE FLUCTUATIONS WITH NORMALIZED RADIAL DISTANCE FROM NOZZLE ORIFICE

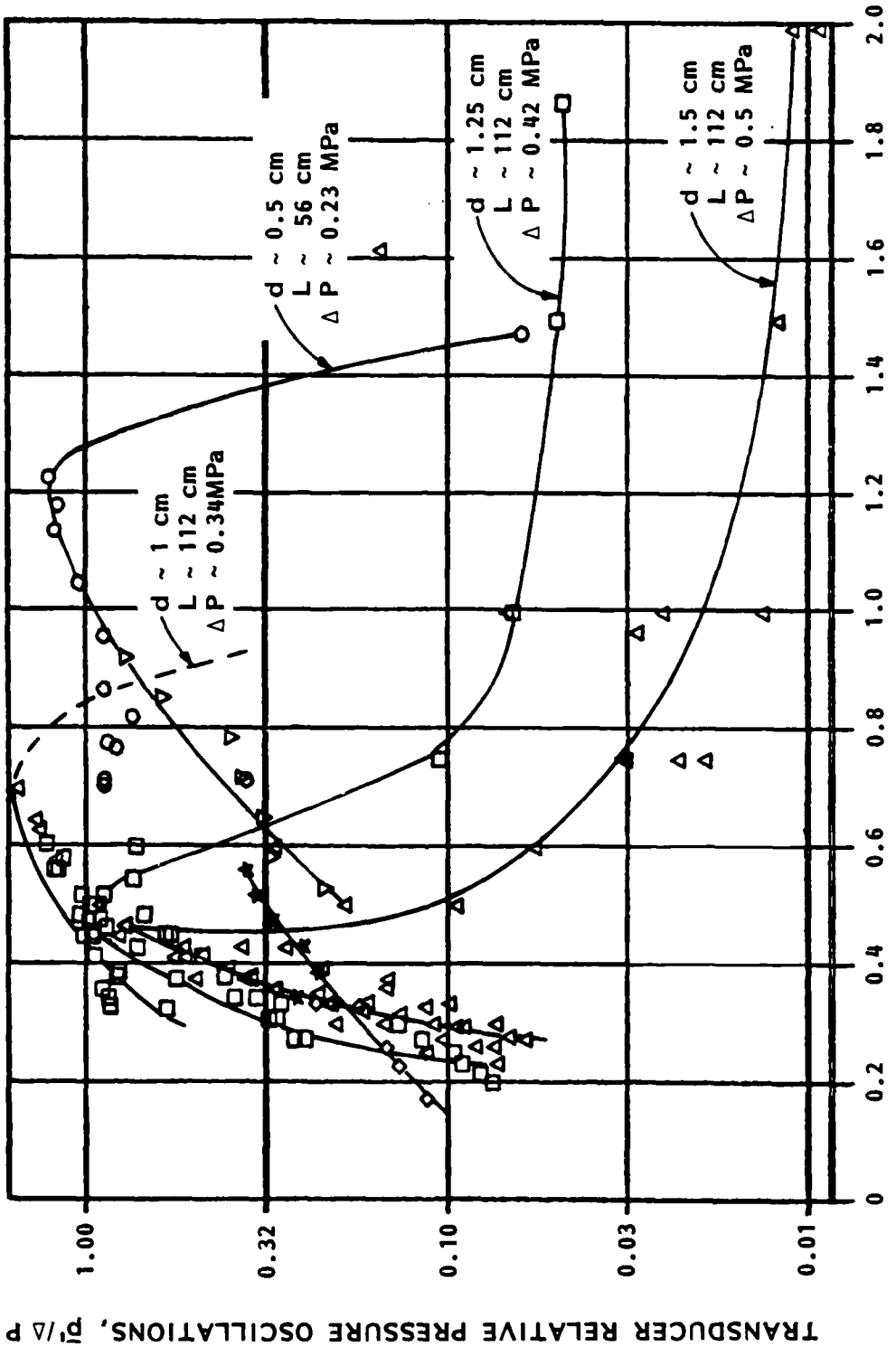

FIGURE 12 - INFLUENCE OF THE CAVITATION NUMBER ON THE RELATIVE PRESSURE FLUCTUATIONS AT MID-LENGTH OF THE ORGAN PIPE FOR VARIOUS NOZZLE DIAMETERS

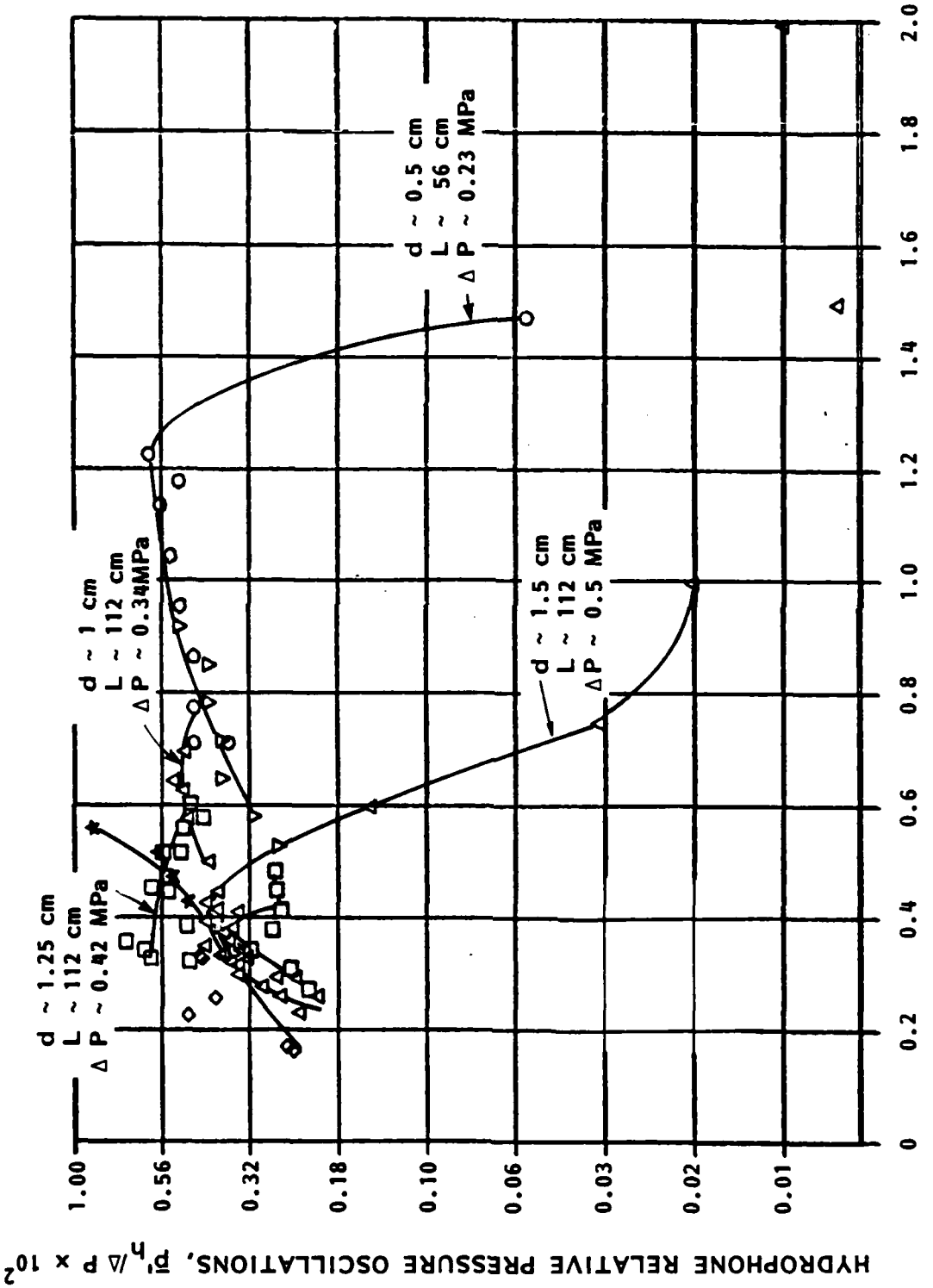

FIGURE 13 - INFLUENCE OF THE CAVITATION NUMBER ON THE RELATIVE PRESSURE FLUCTUATIONS DETECTED BY A HYDROPHONE FOR VARIOUS NOZZLE DIAMETERS. $r \sim 30\ d_j$

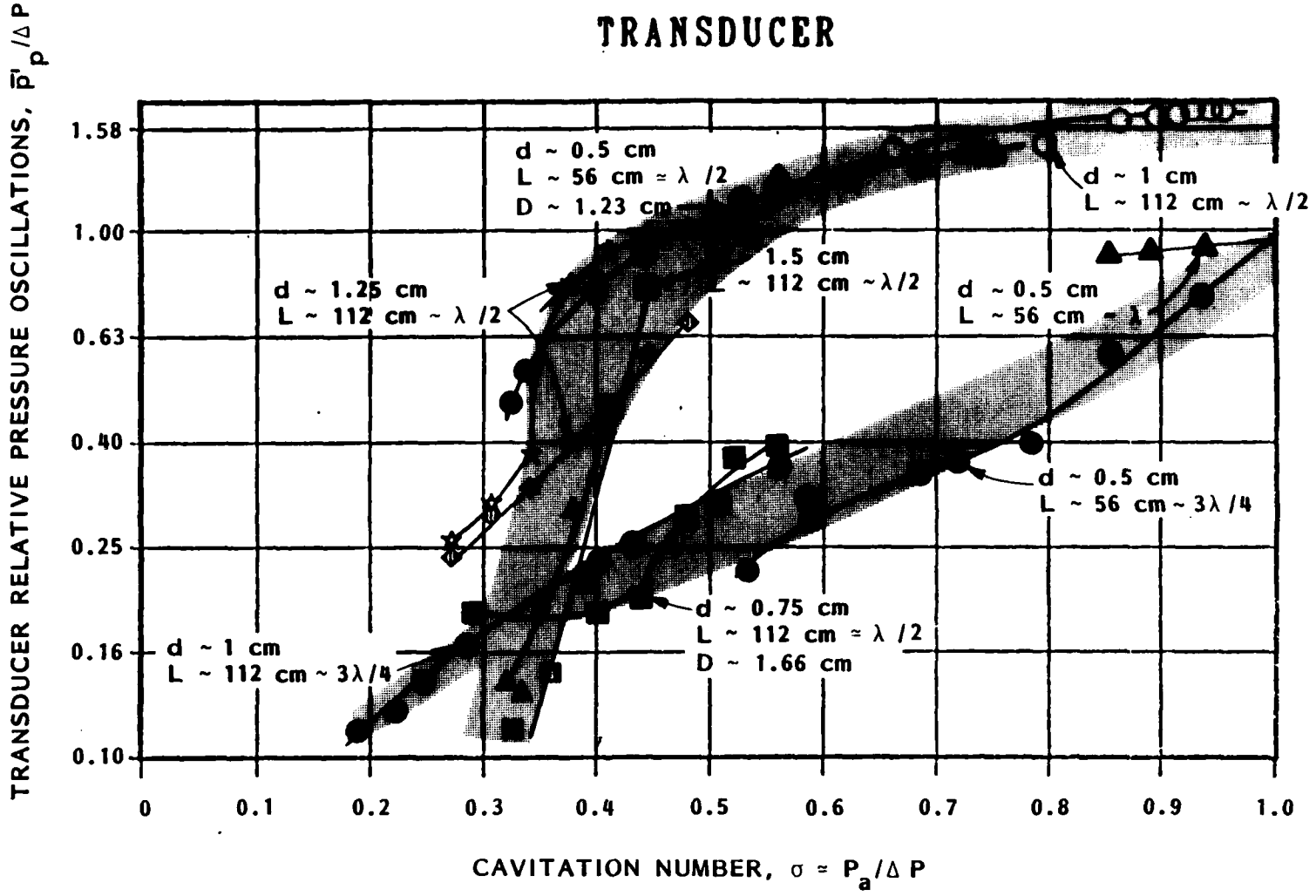

FIGURE 14 - INFLUENCE OF THE CAVITATION NUMBER ON RELATIVE PRESSURE OSCILLATIONS FOR VARIOUS NOZZLE DIAMETERS AND MODES OF OSCILLATION (D ~ 2.5 cm except when noted)

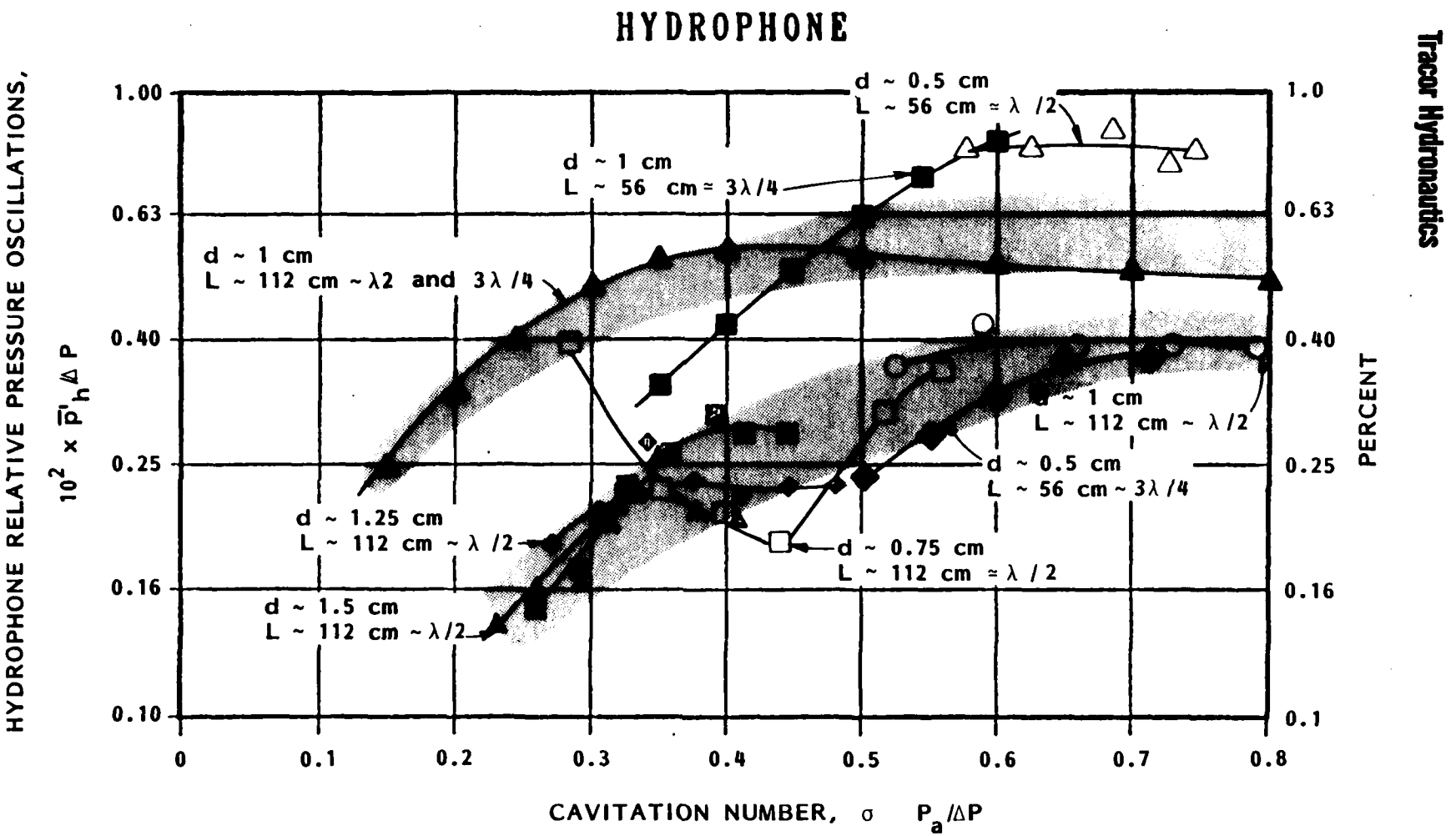

FIGURE 15 - INFLUENCE OF THE CAVITATION NUMBER ON RELATIVE PRESSURE FLUCTUATIONS FOR VARIOUS NOZZLE DIAMETERS AND MODES OF OSCILLATION

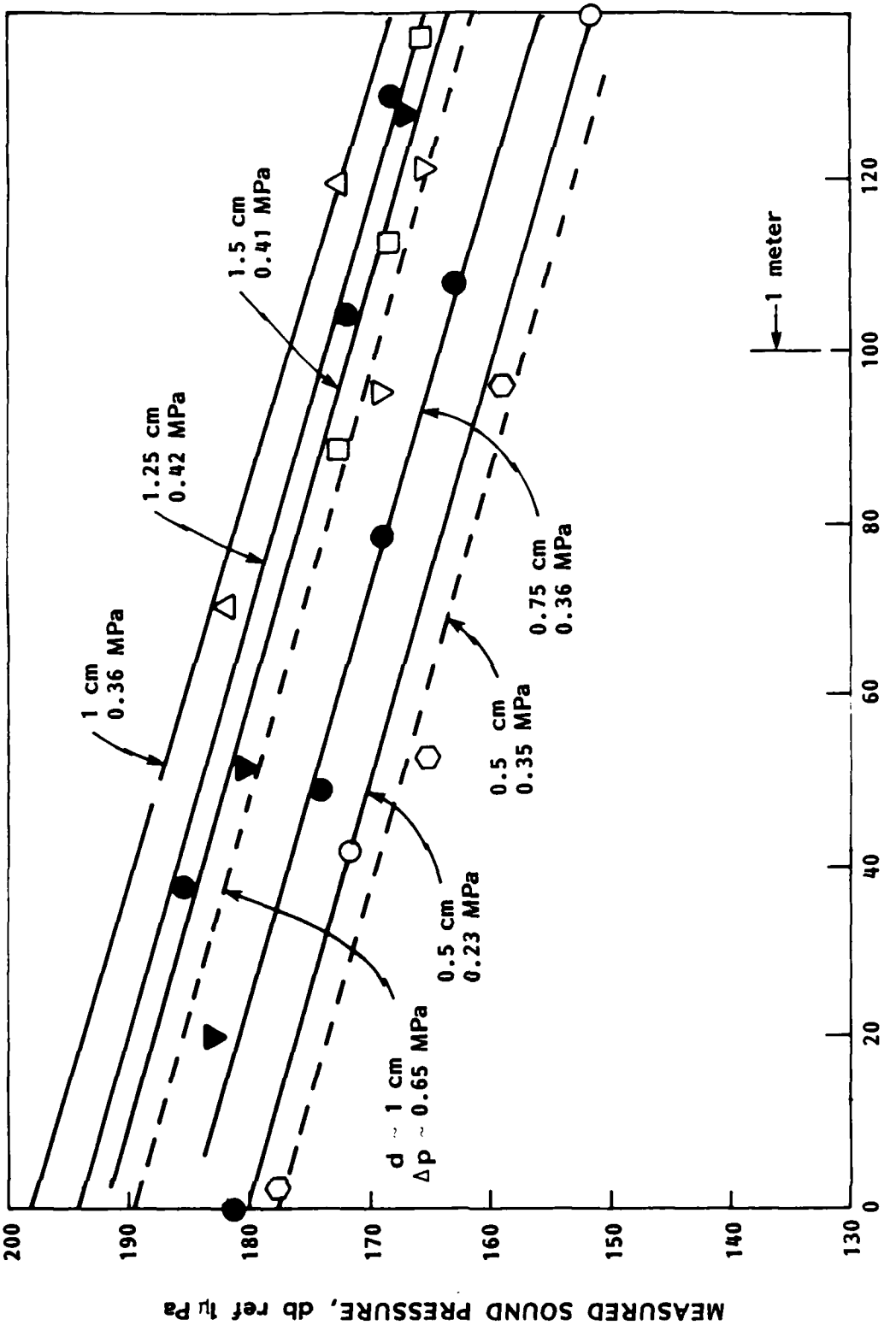

FIGURE 16 - SCALE EFFECTS ON STRATOJET SOUND DECAY WITH DISTANCE FROM THE NOZZLE ORIFICE

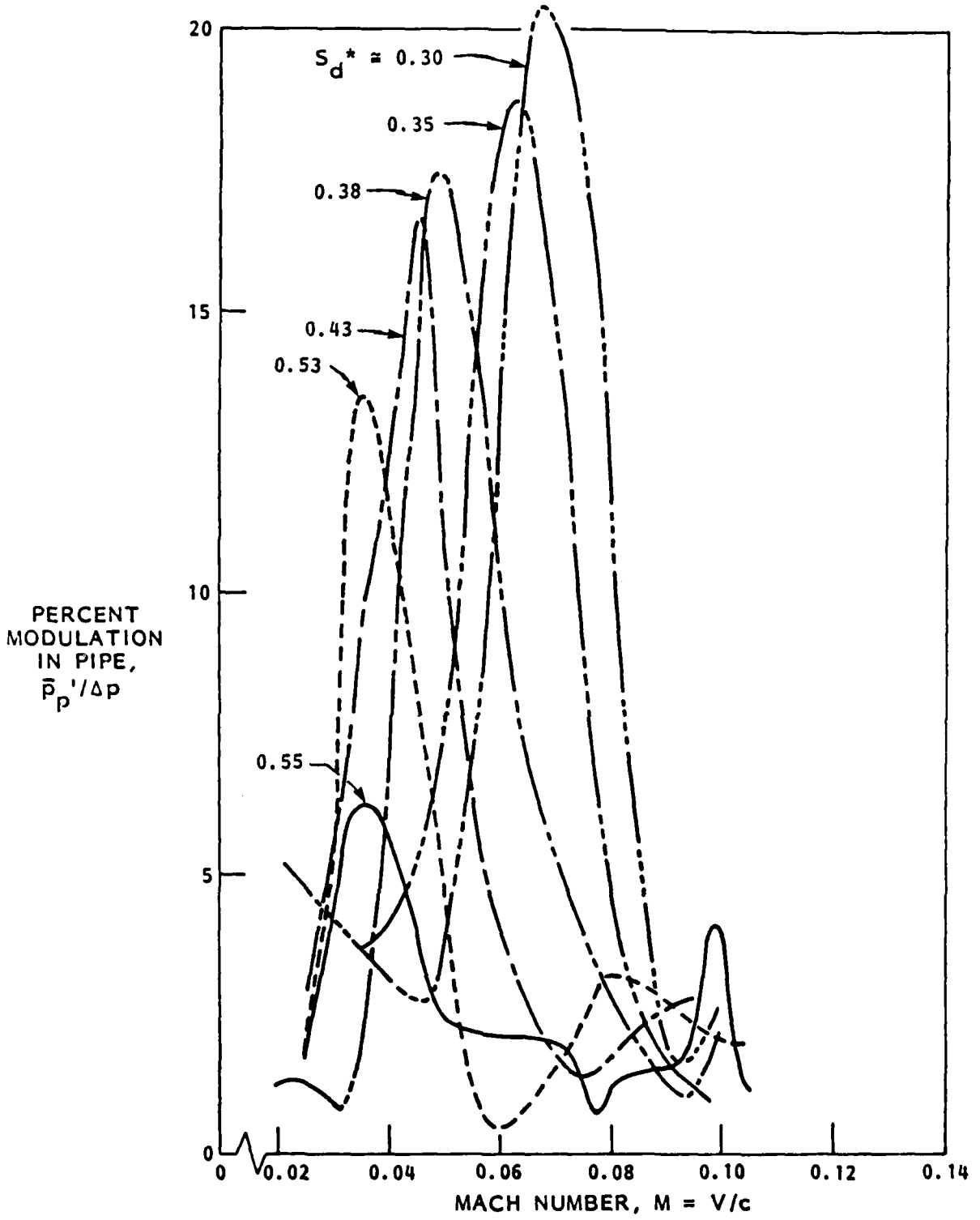

FIGURE 17 - EFFECT OF VARIATIONS IN NOZZLE SHAPE ON ORGAN-PIPE CAVIJET® RESONANCE IN WATER. Nozzle diameter: d = 0.5 cm ; Feed-Tube: straight, diameter: D = 1 cm, length: L_p = 1.72 cm

Variations in the nozzle shape are expressed as changes in the strouhal number at peak oscillations

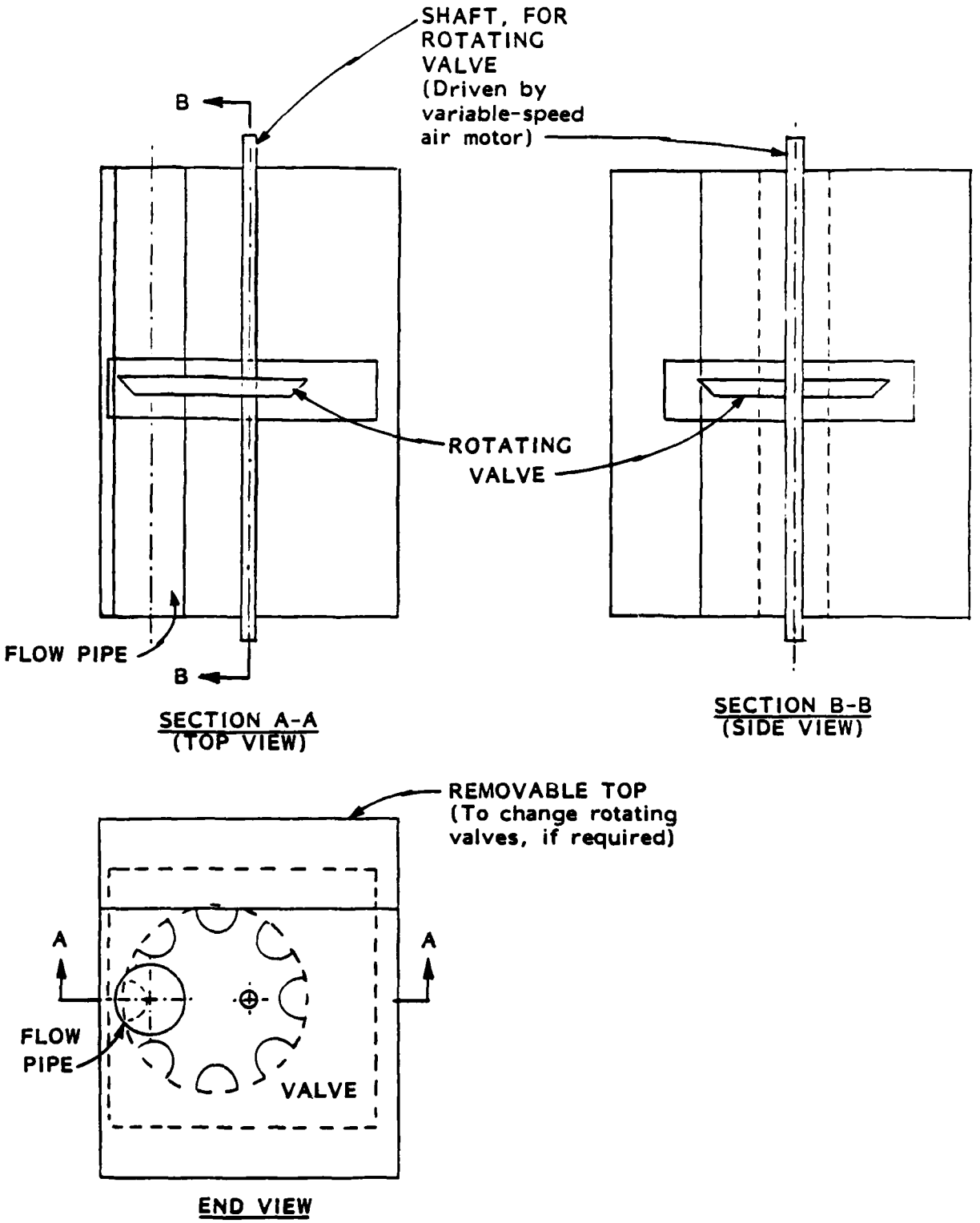

FIGURE 18 - CONCEPT FOR CONTROLLED VARIATION OF FLOW THROUGH STRATOJET NOZZLE

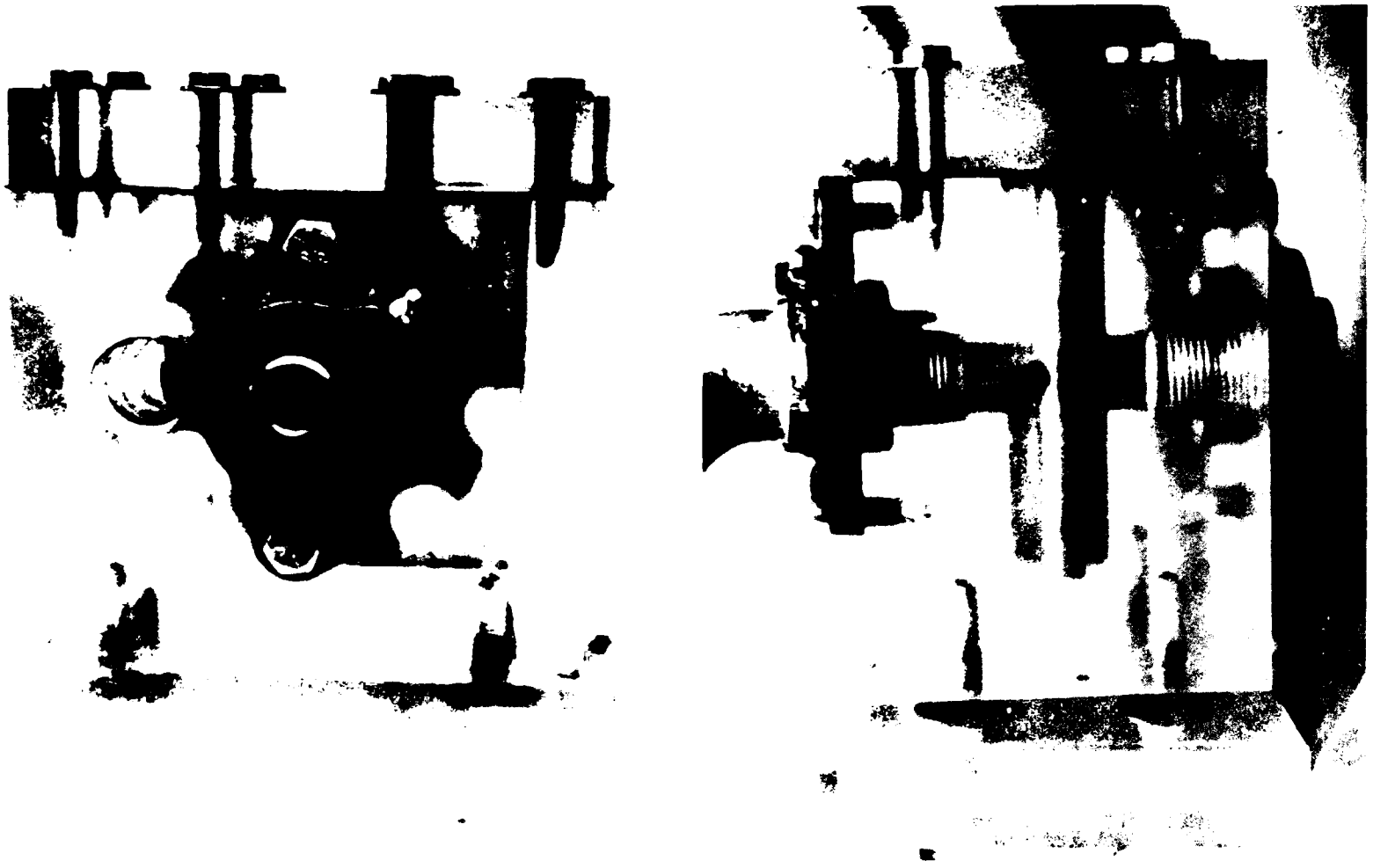

FIGURE 19 FRONT AND SIDE VIEW OF THE CHOPPER

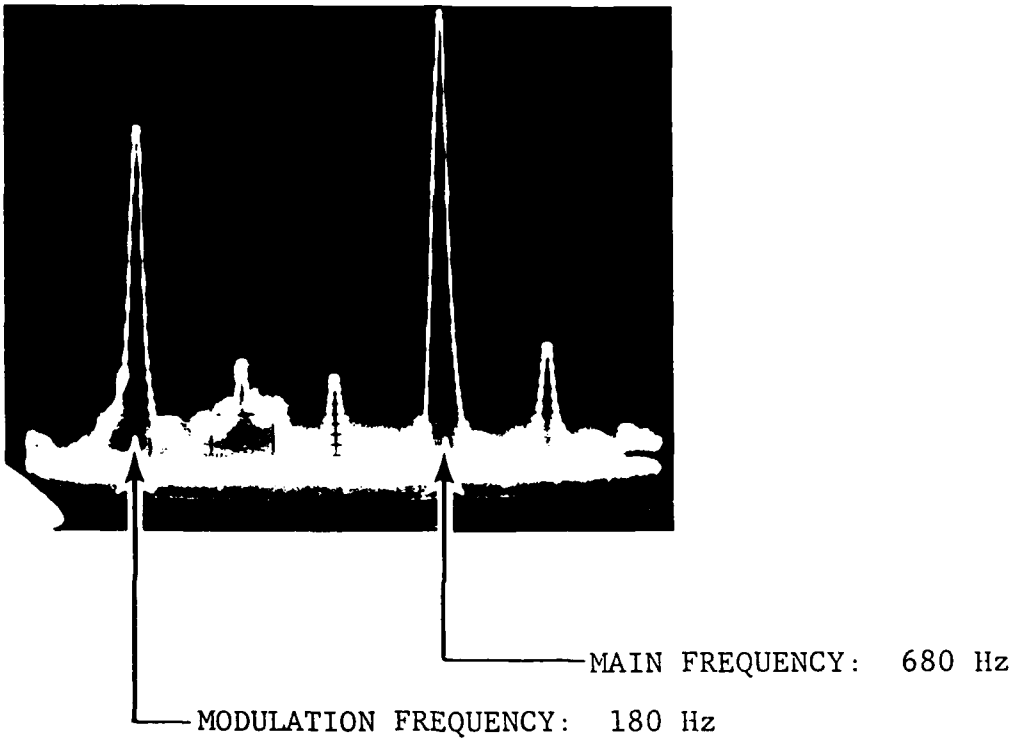

FIGURE 20 - FREQUENCY SPECTRUM OF THE MODULATED SIGNAL EMITTED BY A STRATOJET AND A CHOPPER

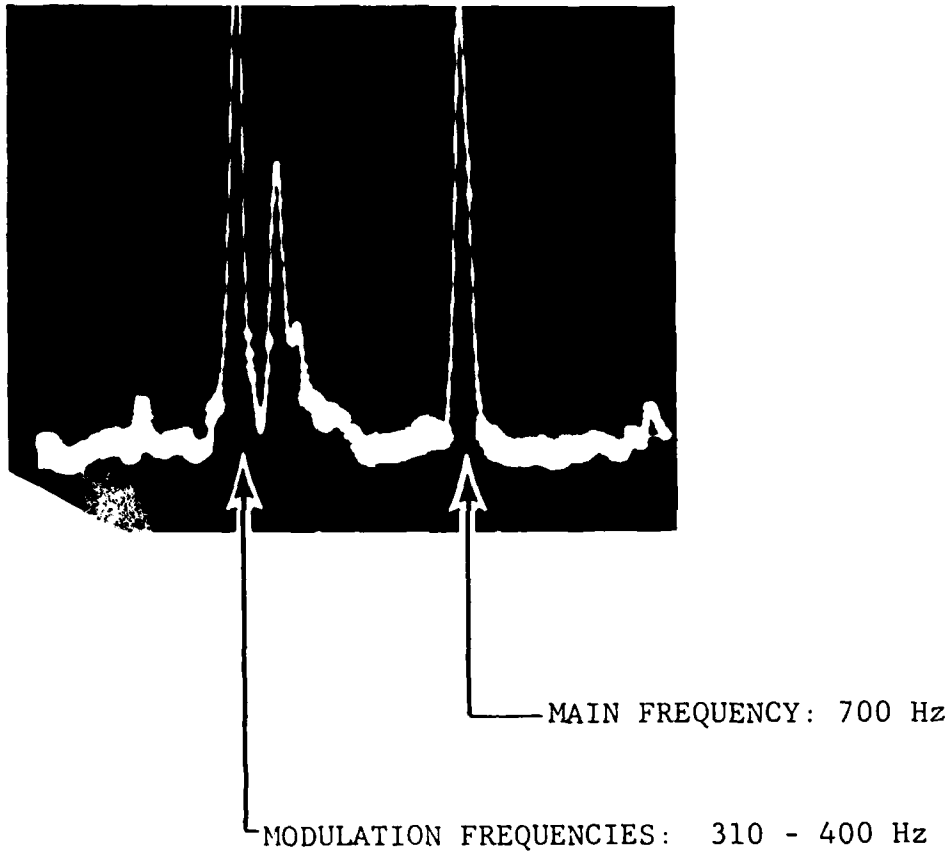

FIGURE 21 - FREQUENCY SPECTRUM OF THE MODULATED SIGNAL EMMITTED BY A STRATOJET AND A CHOPPER

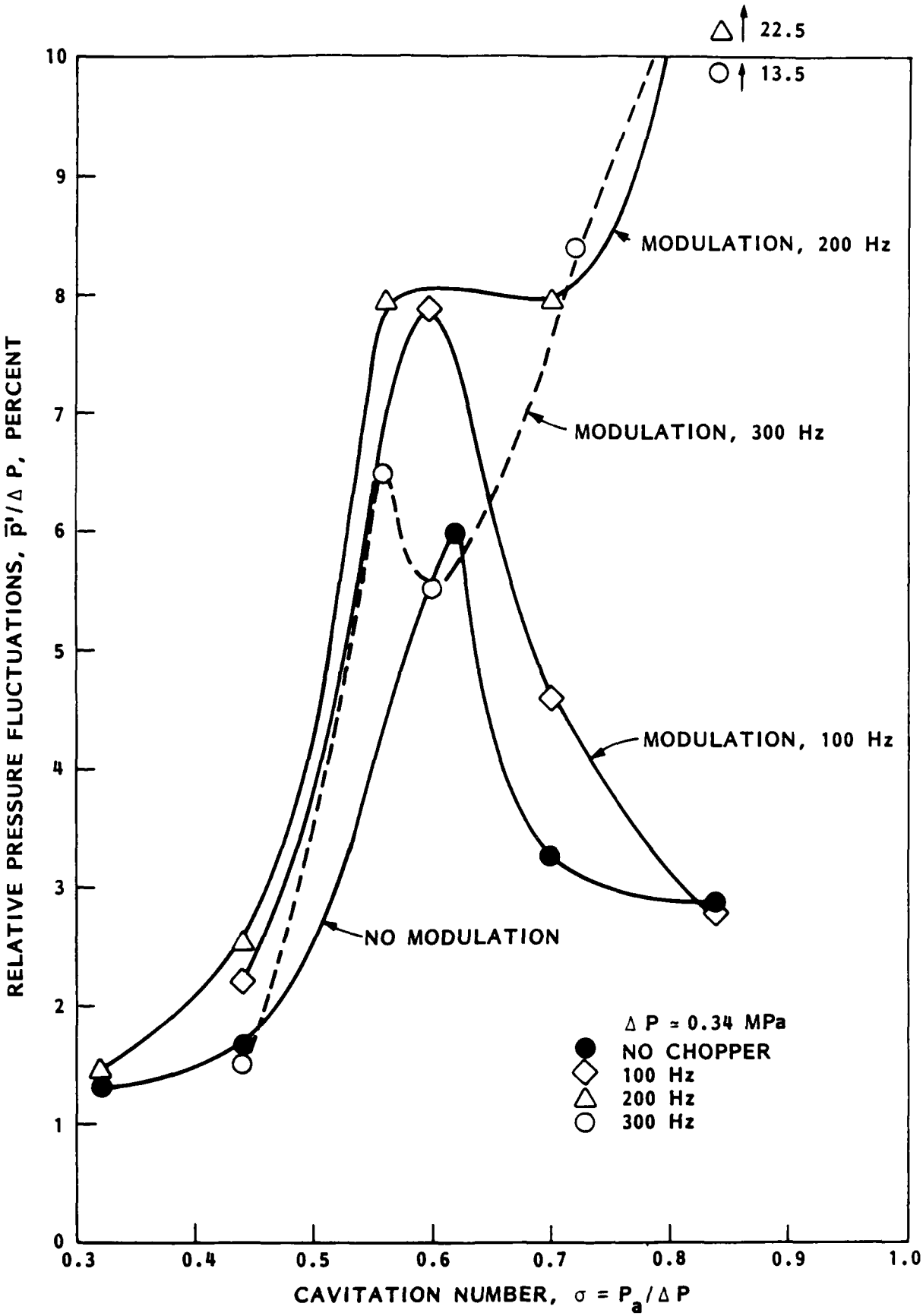

FIGURE 22 - INFLUENCE OF FLOW MODULATION ON RELATIVE PRESSURE FLUCTUATIONS AT MID-LENGTH OF THE ORGAN PIPE. OFF-PEAK TESTS IN THE VISUALIZATION CELL

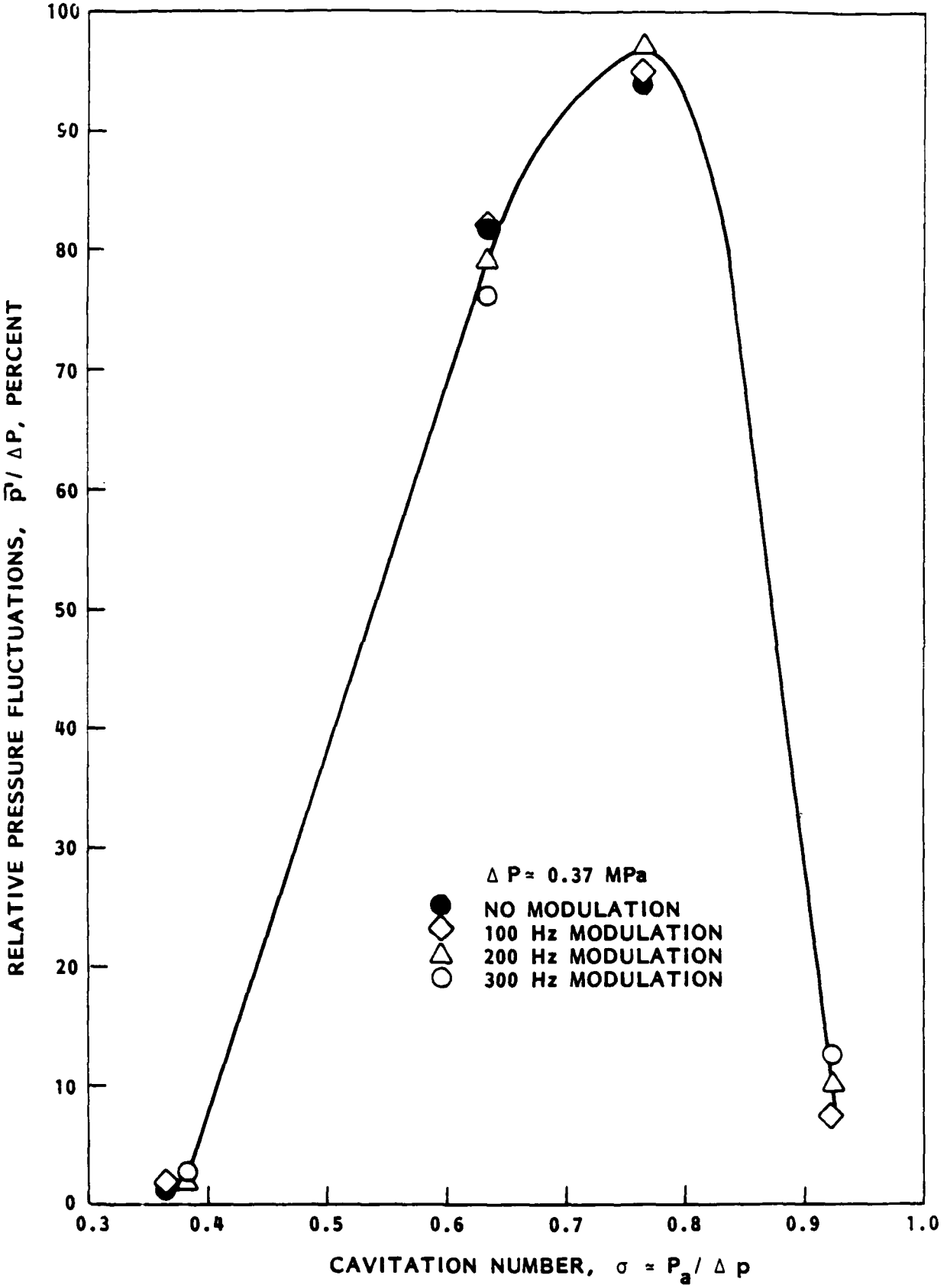

FIGURE 23 - INFLUENCE OF FLOW MODULATION ON RELATIVE PRESSURE FLUCTUATIONS AT MID-LENGTH OF THE ORGAN PIPE. TESTS IN VISUALIZATION CELL AT PEAK MACH NUMBER

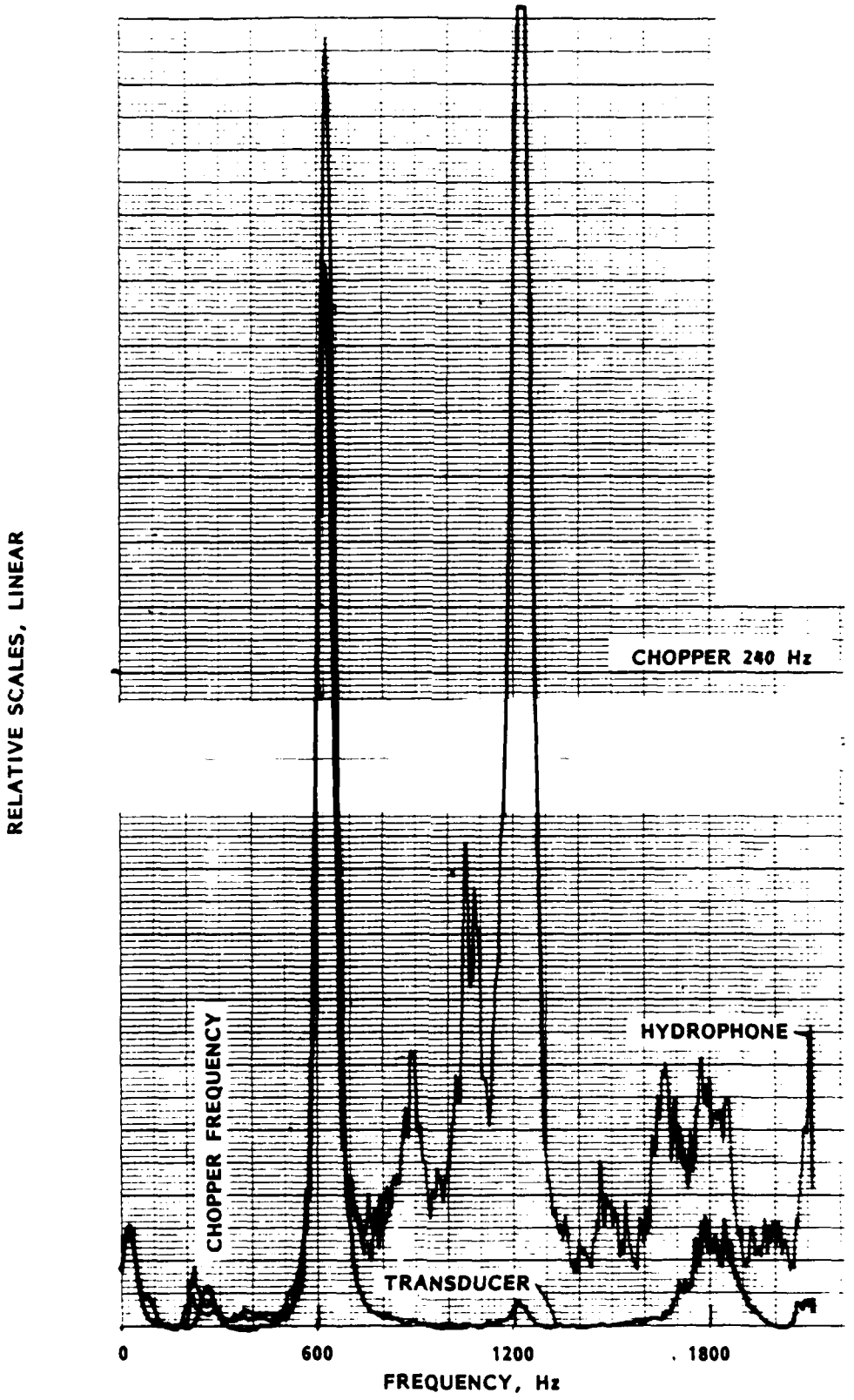

FIGURE 24 - FREQUENCY SPECTRUM OF MODULATED SIGNAL. TEST IN THE DEEP WELL OF THE MODEL BASIN. f = 240 Hz

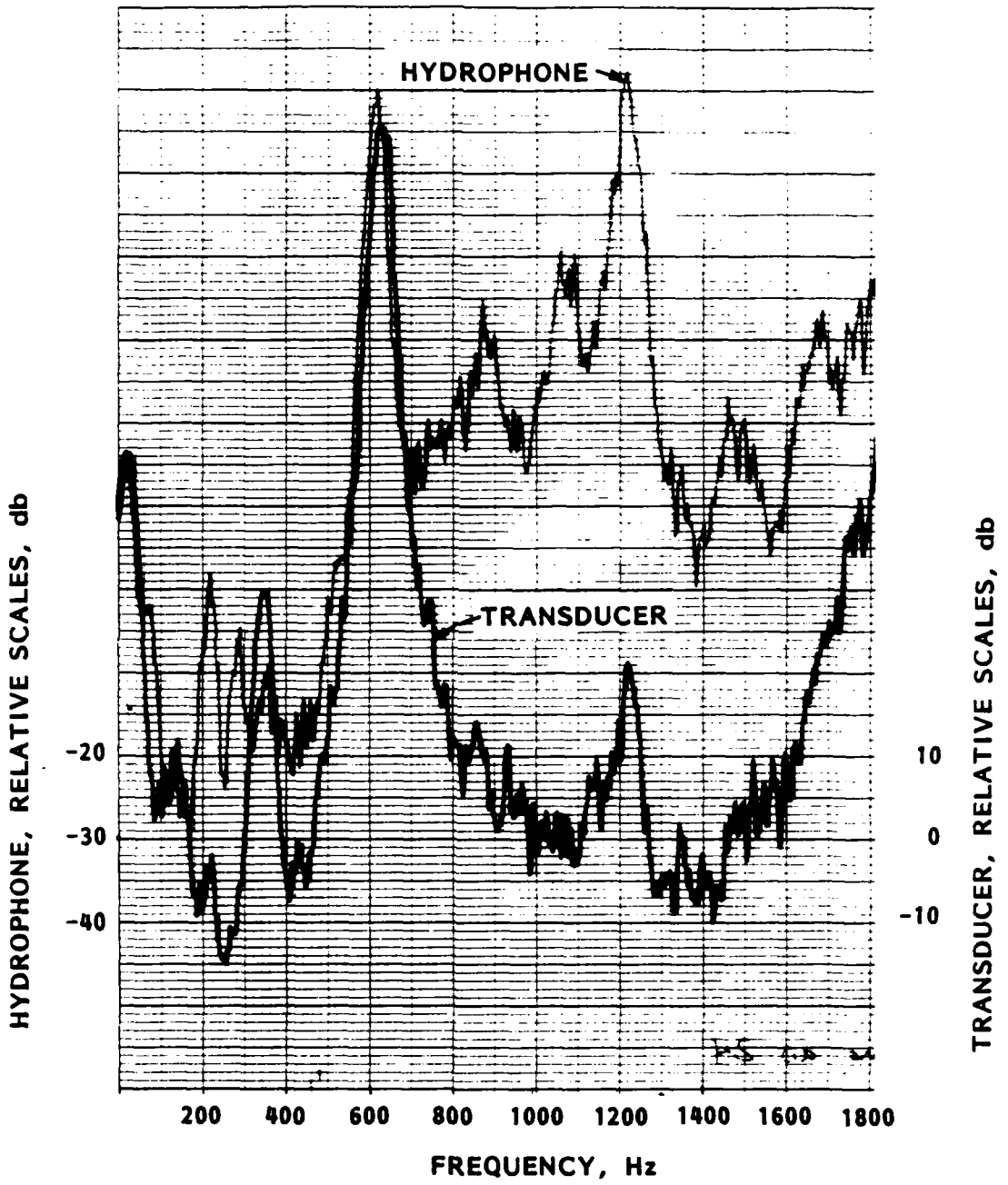

FIGURE 25 - FREQUENCY SPECTRUM OF MODULATED SIGNAL.
TEST IN THE DEEP WELL OF THE MODEL BASIN.
f = 330 Hz

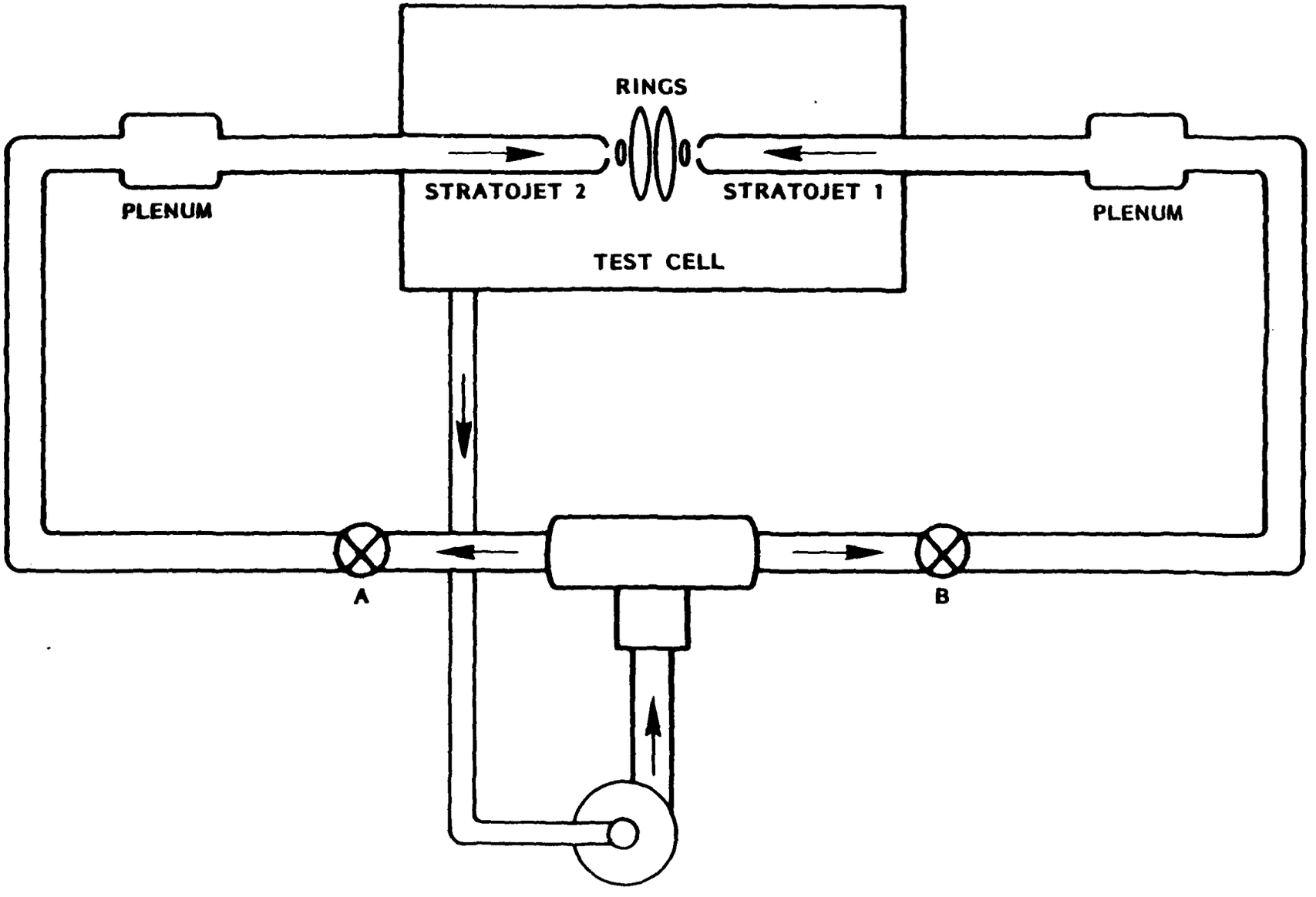

FIGURE 26 - SCHEMATIC OF OPPOSING JET EXPERIMENT SET-UP FACILITY

FIGURE 27 - INTERACTION BETWEEN OPPOSING STRATOJETS. A SLIGHT ASYMMETRY IN GEOMETRY HAS INDUCED AN INCLINATION OF THE STRETCHING PLANE AND A DISPLACEMENT OF THE STAGNATION POINT TOWARDS ONE OF THE NOZZLES

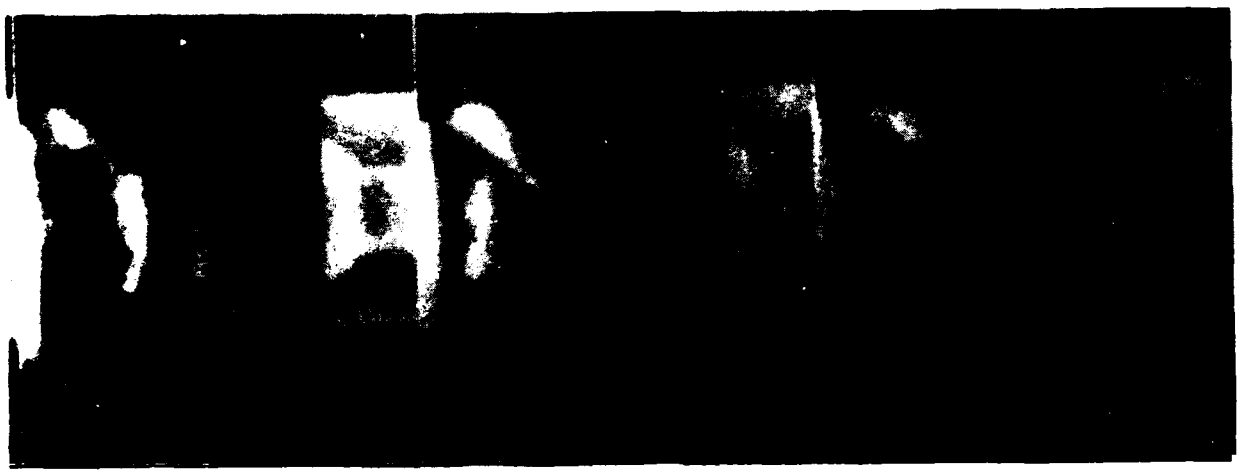

FIGURE 28 - INTERACTION BETWEEN OPPOSONG STRATOJETS. A SLIGHT ASYMMETRY HAS INDUCED AN INCLINATION OF THE STRETCHING PLANE.

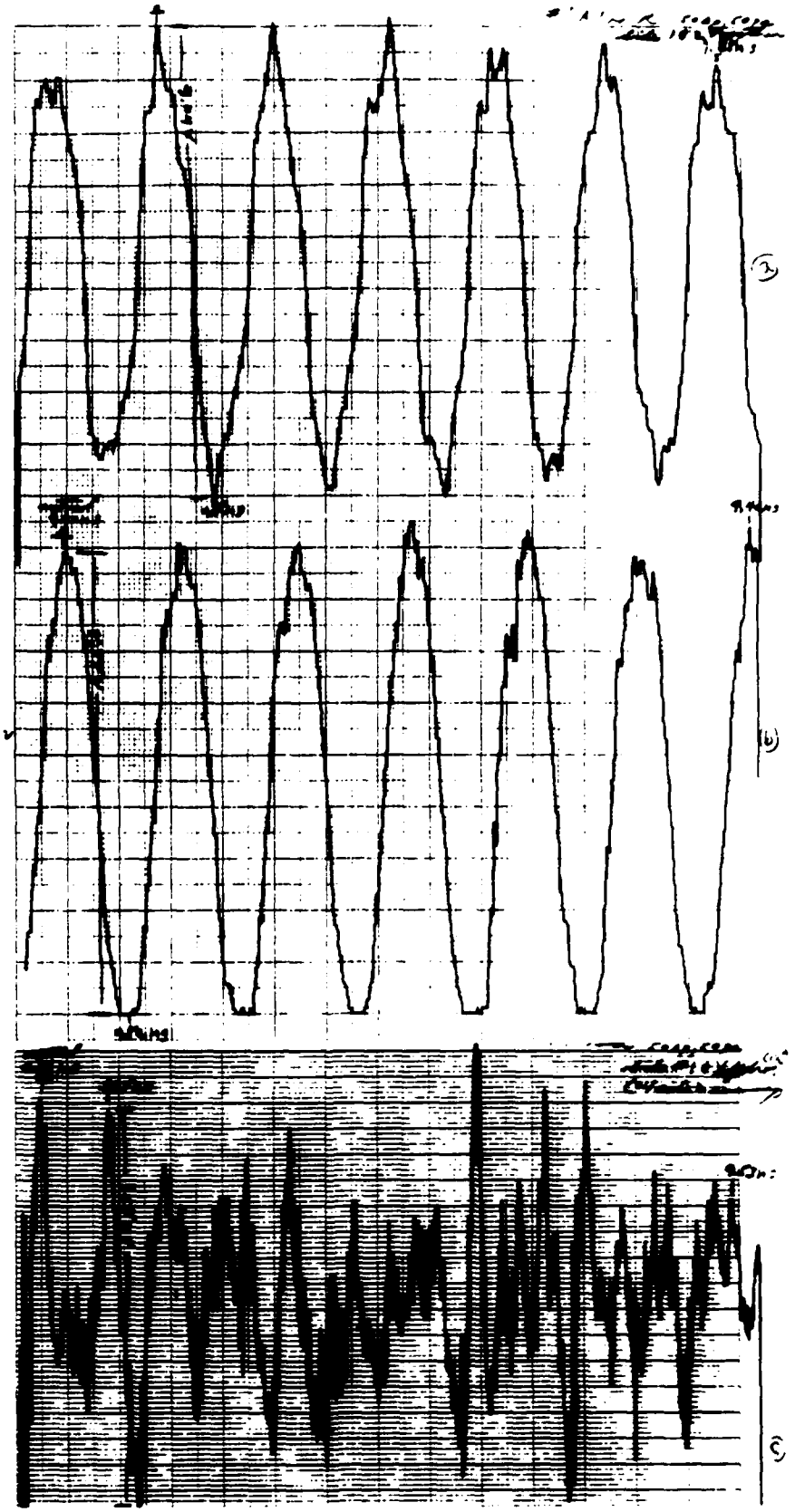

FIGURE 29 - PRESSURE FLUCTUATIONS SIGNALS: TRANSDUCER AT MID LENGTH OF FIRST AND SECOND STRATOJET AND HYDROPHONE AT 1.5 in. FROM CENTERLINE. $\Delta P = 0.34$ MPa $P_a = 0.34$ MPa, NOZZLES SEPARATION DISTANCE = 5 cm

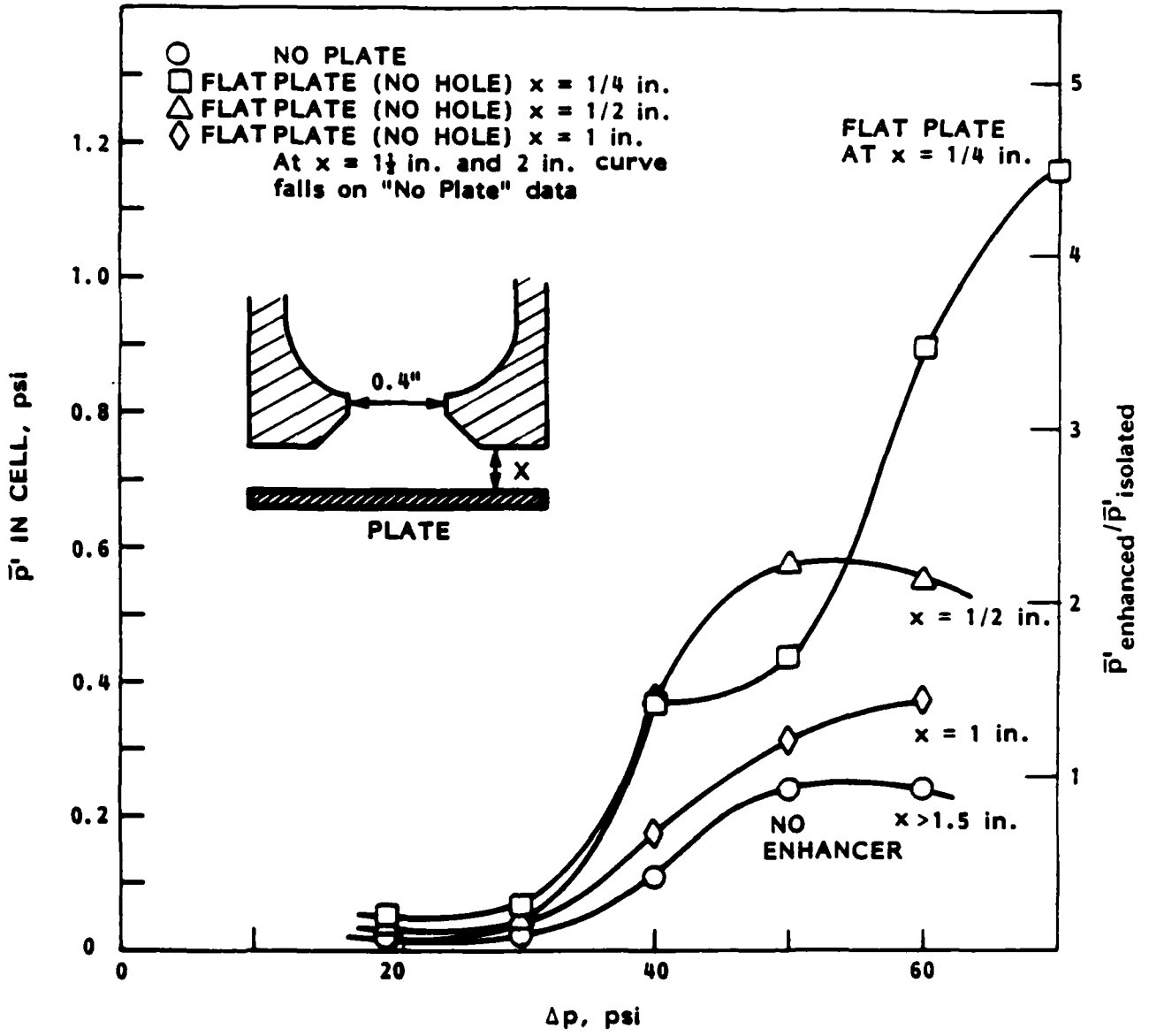

FIGURE 30 - NOISE ENHANCEMENT WITH AN IMPACTED PLATE
P_a = 30 psi, d = 0.40 in.,

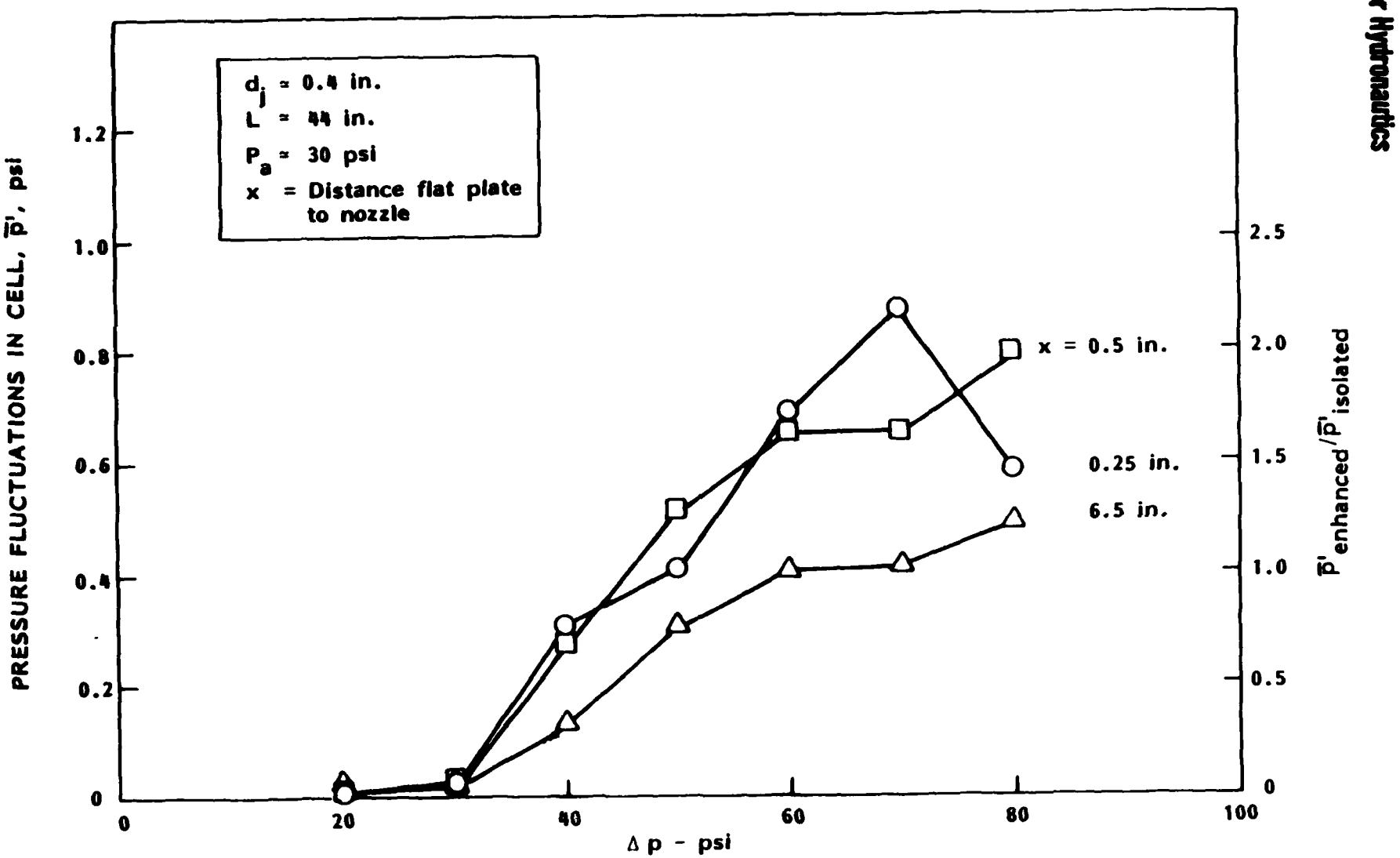

FIGURE 31 - NOISE ENHANCEMENT WITH A FLAT IMPACTED PLATE. AVERAGE VALUES FROM REPEATED TESTS. HYDROPHONE AT 3.5 in. FROM JET AXIS AND 0.5 in. ABOVE NOZZLE EXIT PLANE.

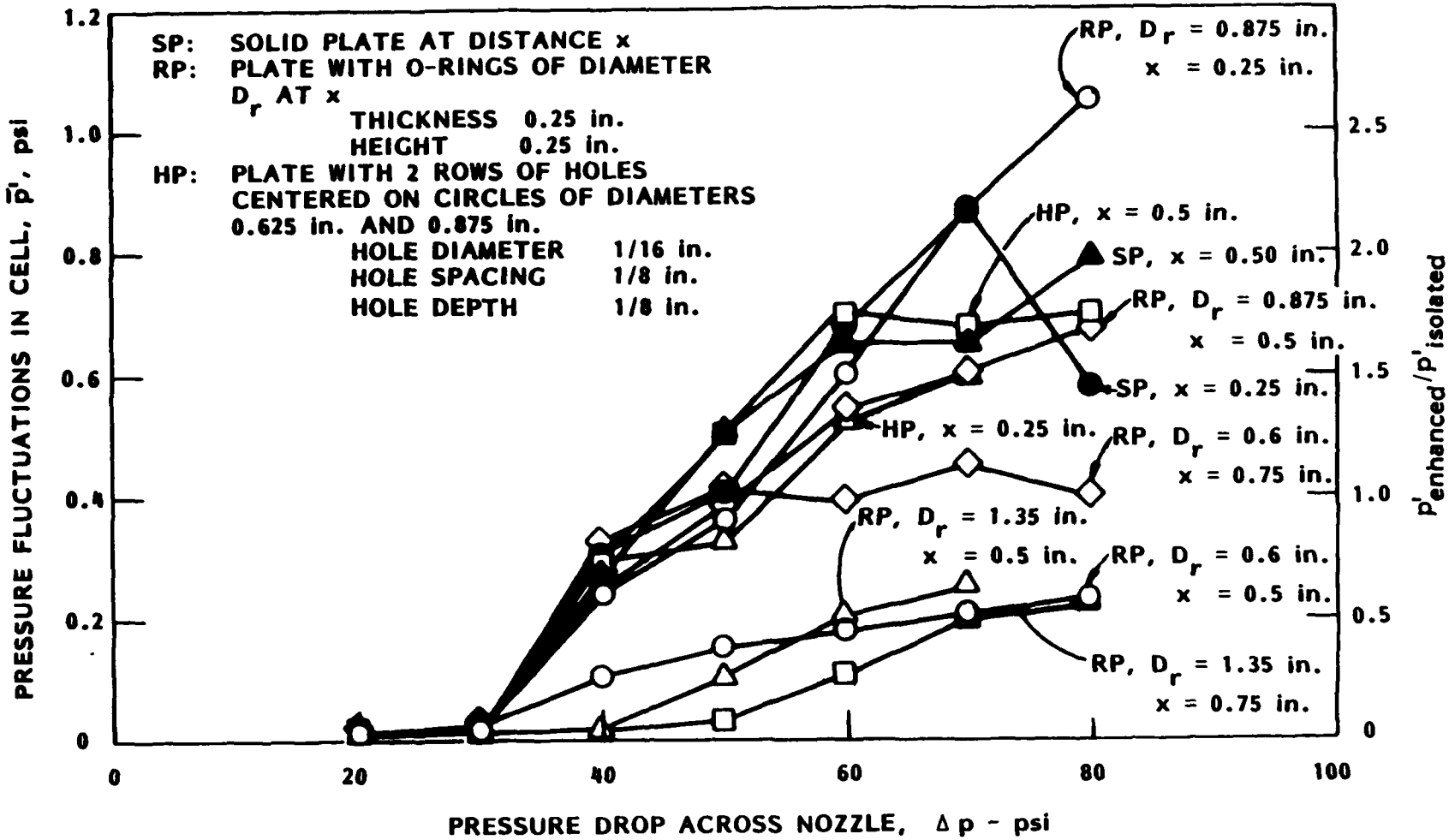

FIGURE 32 - NOISE ENHANCEMENT USING AN IMPACTED FLAT PLATE WITH VARIOUS OBSTACLES ON THE PLATE. HYDROPHONE AT 3.5 in. FROM JET AXIS AND 0.5 in. ABOVE NOZZLE EXIT PLANE

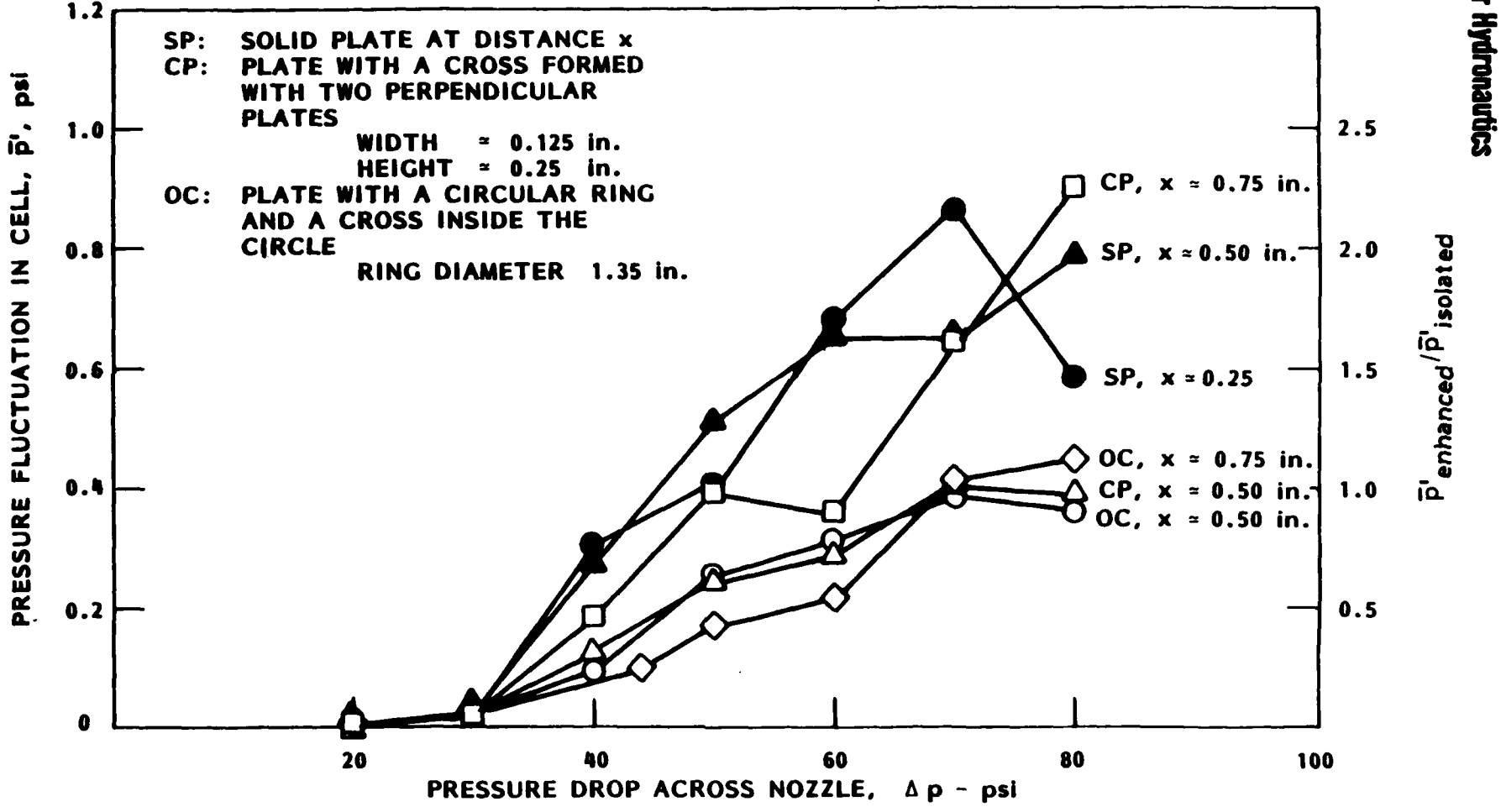

FIGURE 33 - NOISE ENHANCEMENT USING AN IMPACTED FLAT PLATE WITH VARIOUS OBSTACLES ON THE PLATE. HYDROPHONE AT 3.5 in. FROM JET AXIS AND 0.5 in. ABOVE NOZZLE EXIT PLANE

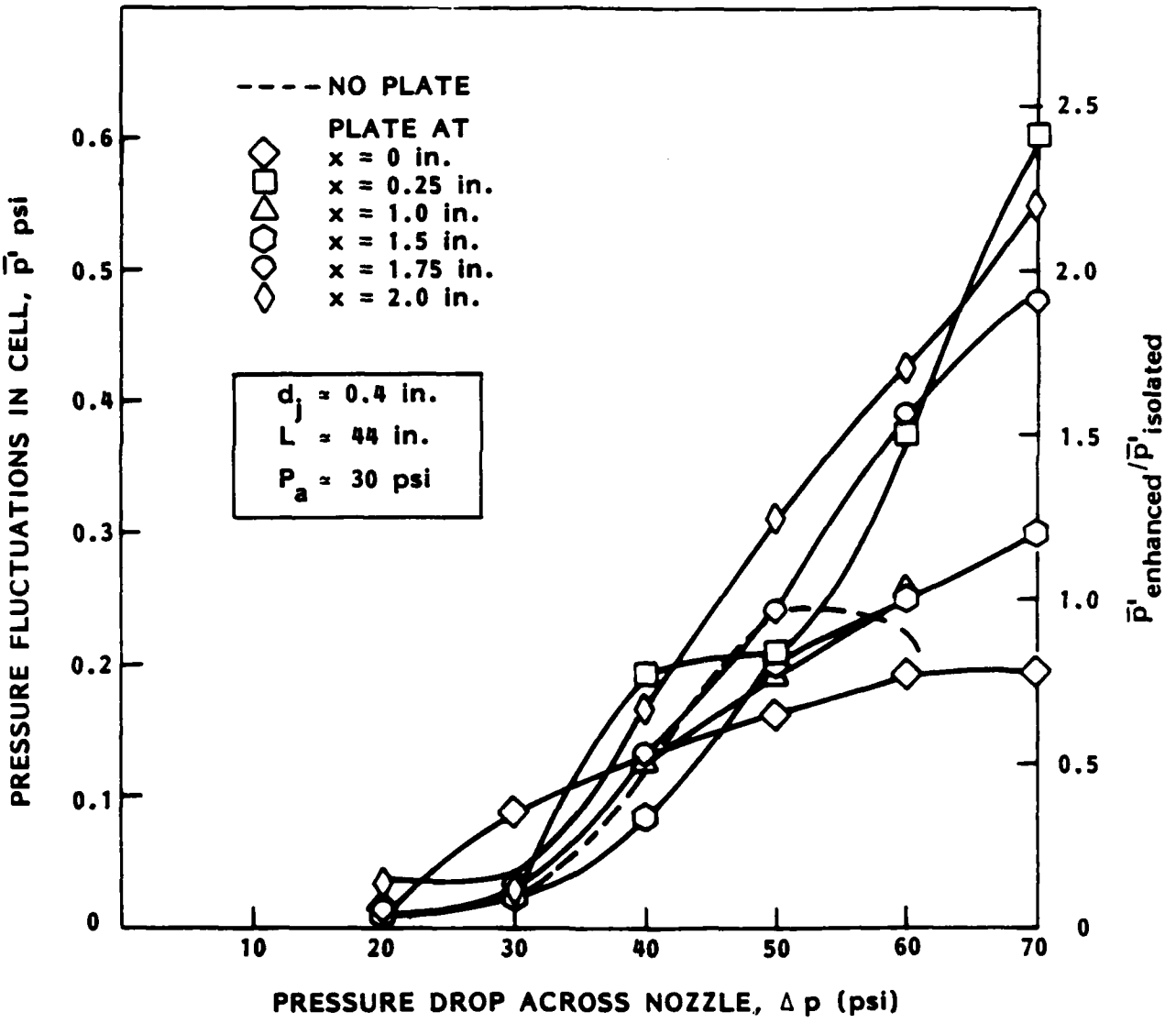

FIGURE 34 - NOISE ENHANCEMENT USING A FLAT PLATE WITH A CENTERED CIRCULAR HOLE 0.5 in. DIAMETER. HYDROPHONE 3.5 in. FROM JET AXIS, 0.5 in. ABOVE NOZZLE EXIT PLAN

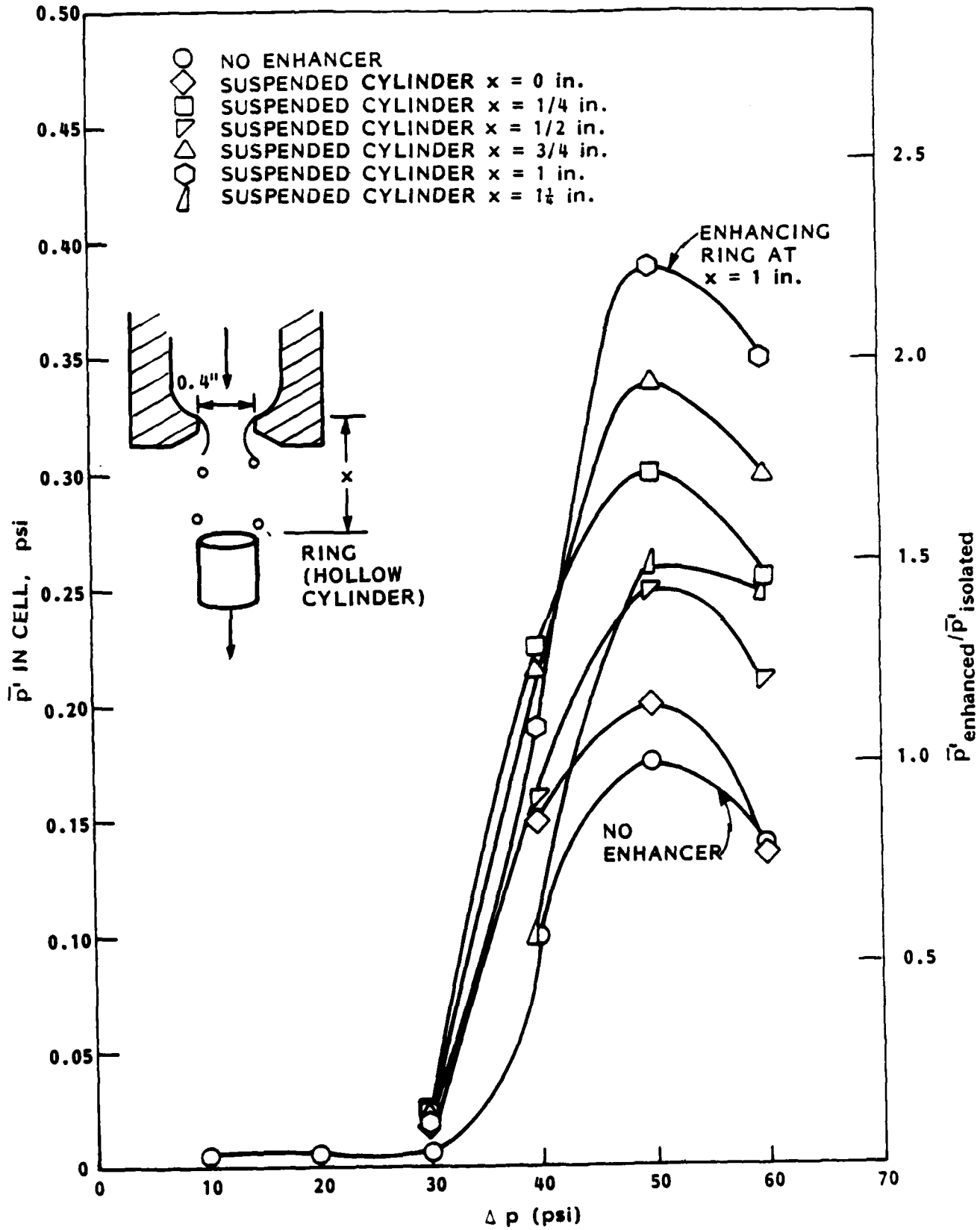

FIGURE 35 - NOISE ENHANCEMENT WITH A HOLLOW CYLINDER (RING)
P_a = 30 psi, d = 0.4 in., CYLINDER = I.D. ~ 0.41 in.,
O.D. ~ 0.5 in., L ~ 0.21 in.

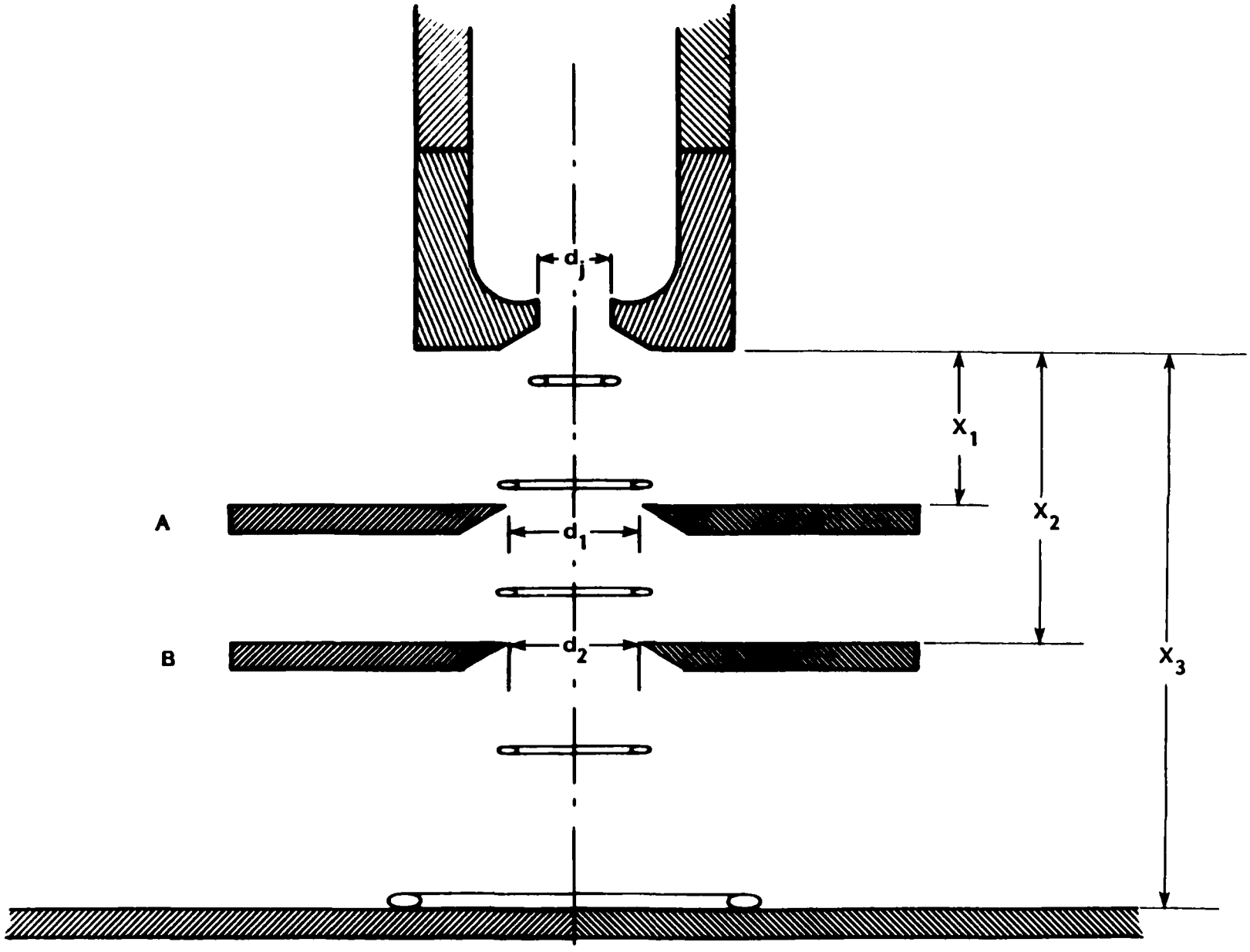

FIGURE 36 - DUAL ORIFICE RESONATOR ENHANCER. SCHEMATIC OF GEOMETRIC CHARACTERISTICS

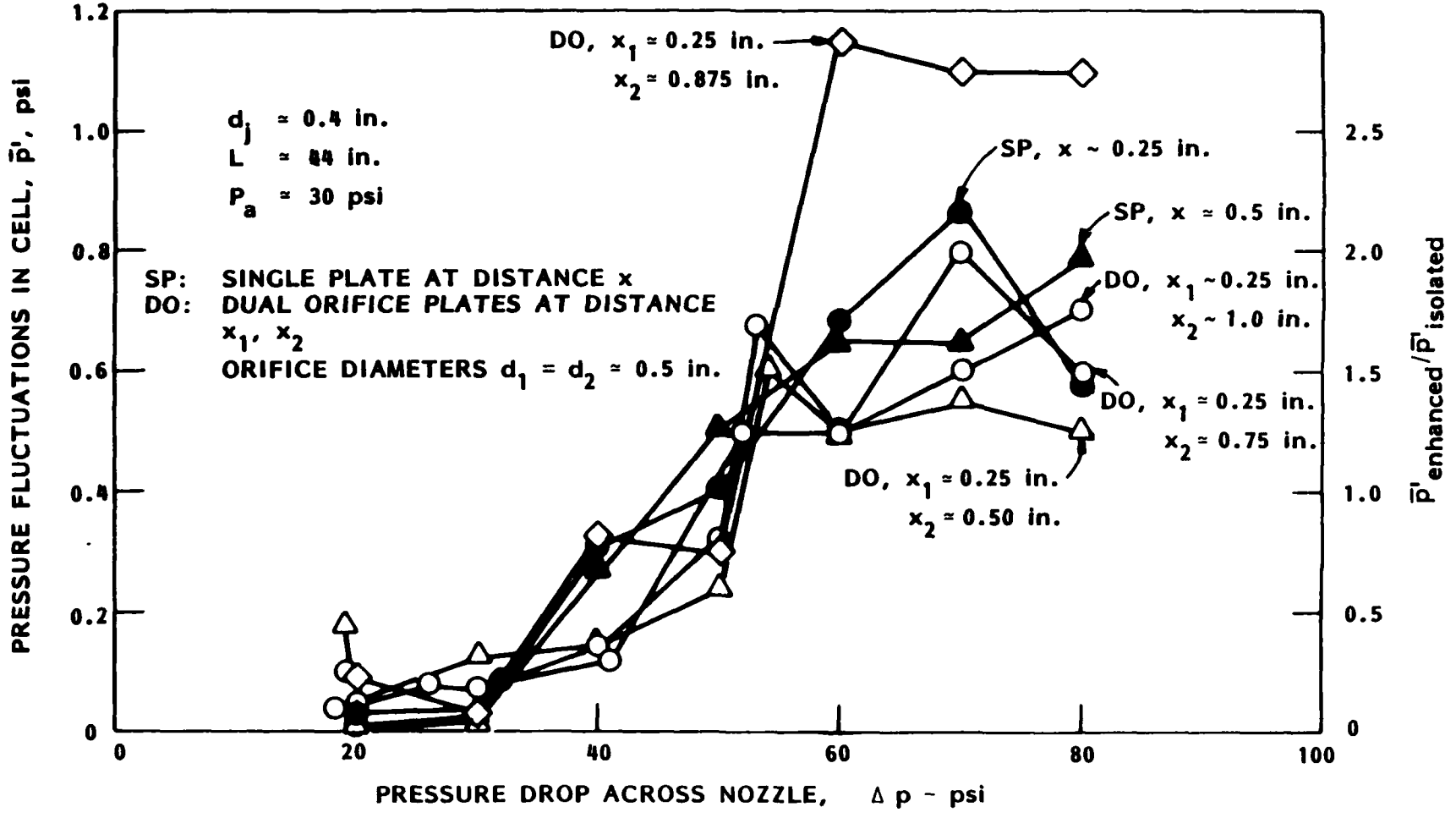

FIGURE 37 - STRATOJET NOISE ENHANCEMENT USING A DUAL ORIFICE RESONATOR

a. b. c.

a. $\Delta P \simeq 70$ psi, $P_a \sim 30$ psi, $d_j \sim 0.4$ in., $d_1 = d_2 \simeq 0.562$ in.
$X_1 = 0.25$ in., $X_2 = 0.875$ in., $p' \sim 1.25$ psi, no plate

b. and c. $\Delta P \simeq 60$ psi, $P_a \sim 30$ psi, $d_j \sim 0.4$ in., $d_1 = d_2 \simeq 0.562$ in.,
$X_1 = 0.25$ in., $X_2 = 0.875$ in., $p' \simeq 1.48$ psi, no plate

FIGURE 39 - PICTURES OF THE INTERACTION BETWEEN A STRATOJET AND A DUAL ORIFICE EHNHANCER

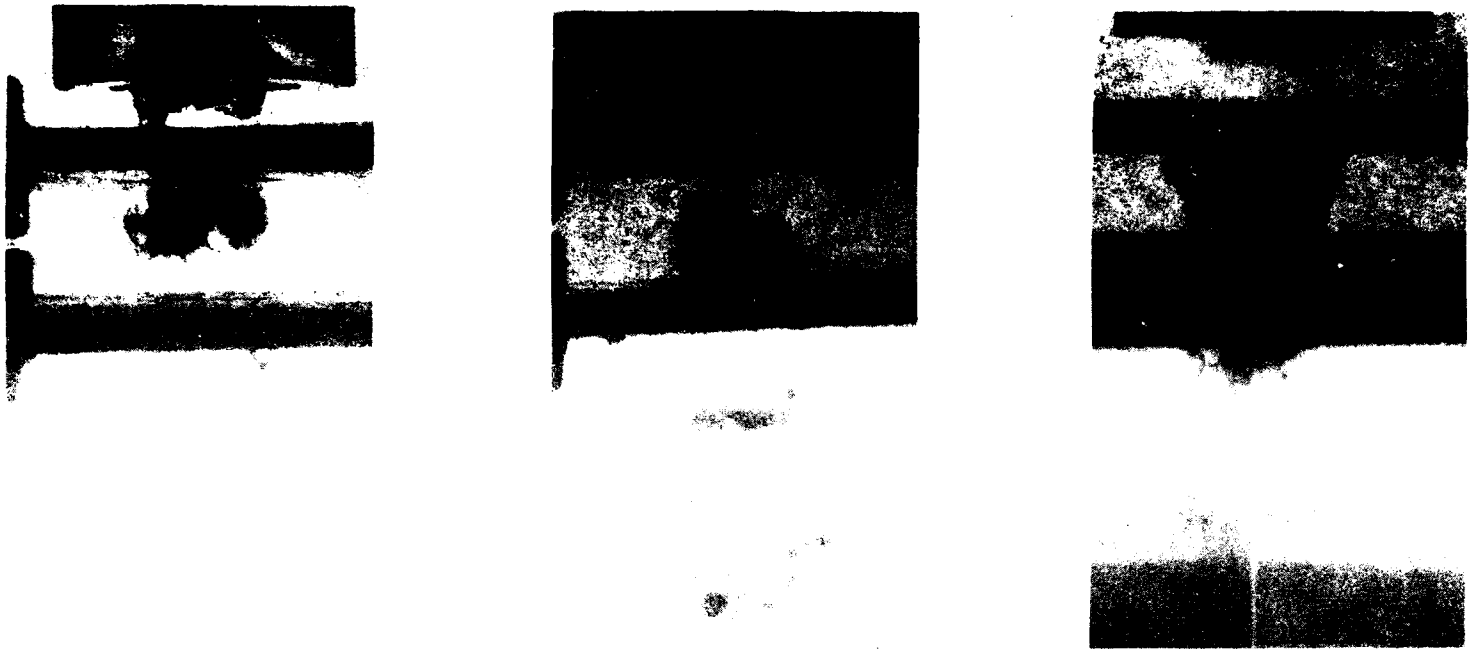

a. b. c.

a. and b. $\Delta P = 70$ psi, $P_a \sim 30$ psi, $d_j \sim 0.4$ in., $d_1 = d_2 \simeq 0.562$ in., $X_1 = 0.25$ in., $X_2 \simeq 0.875$ in., $p' \sim 1.25$ psi, no plate

c. $\Delta P = 70$ psi, $P_a \sim 30$ psi, $d_j \sim 0.4$ in., $d_1 = d_2 \sim 0.562$ in., $p' \simeq 1.40$ psi, plate at $X \sim 2.5$ in.

FIGURE 38 - PICTURES OF THE INTERACTION BETWEEN A STRATOJET AND A DUAL ORIFICE ENHANCER

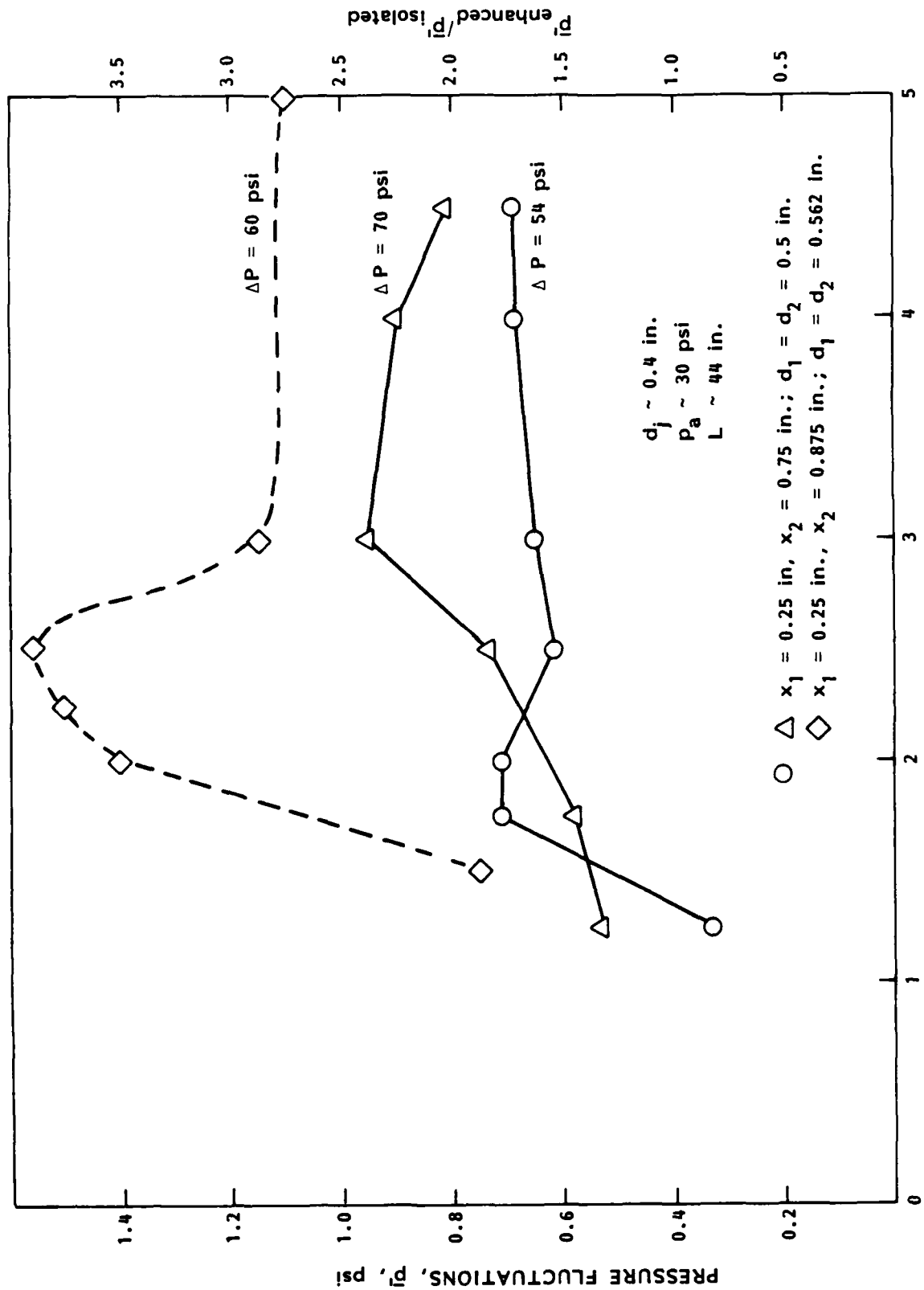

FIGURE 40 - INFLUENCE OF THE DISTANCE FROM AN IMPACTED PLATE ON A STRATOJET DUAL OFICIE COMBINATION NOZZLE GENERATION CABILITY

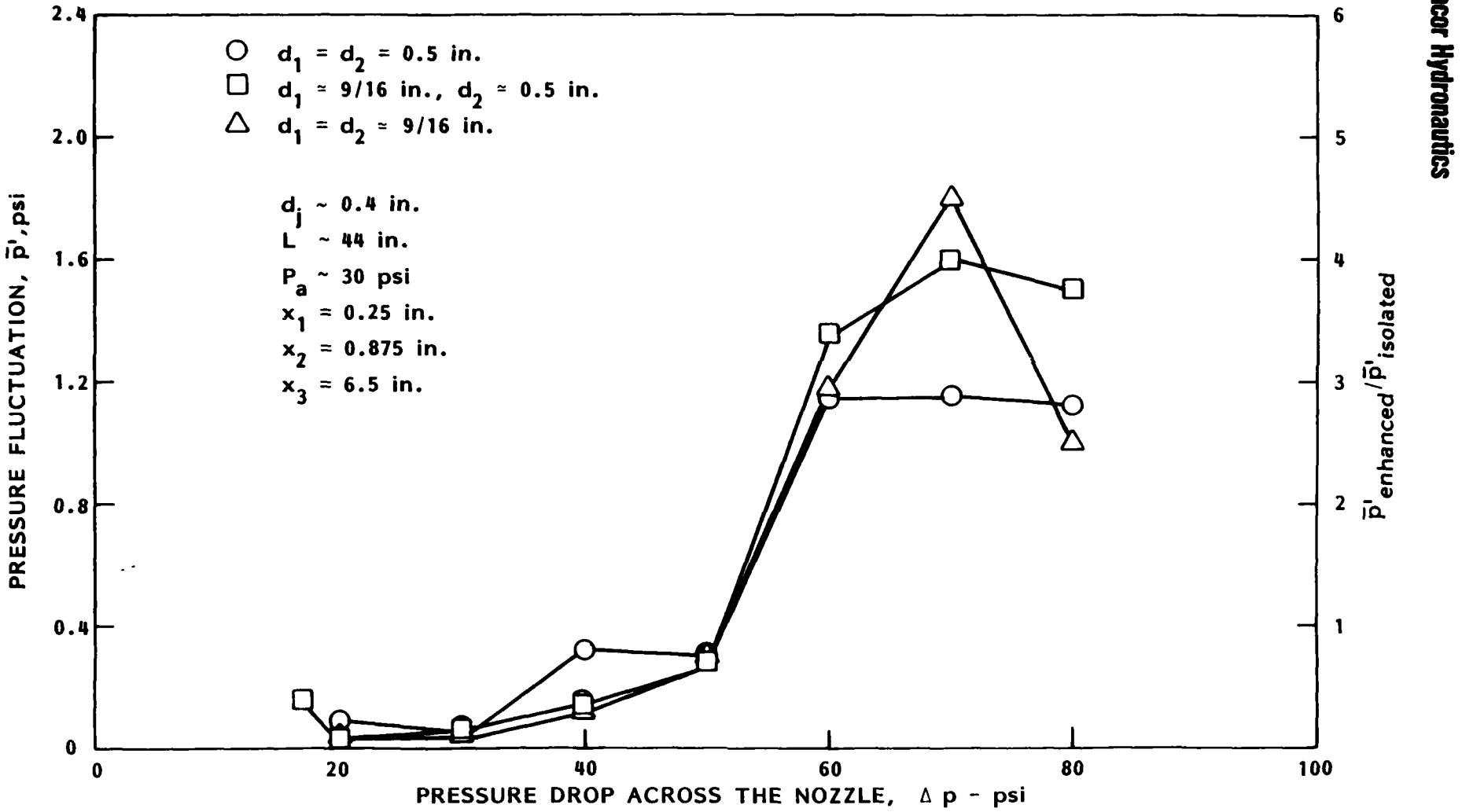

FIGURE 41 - INFLUENCE OF THE PRESSURE DROP ACROSS THE NOZZLE ON THE NOISE GENERATION OF A DUAL ORIFICE STRATOJET COMBINATION

END

FILMED

6-86

DTIC